~4:1 ratio. After standing overnight at room temperature, similar NMR analysis showed complete disappearance of the downfield resonance.

Exchange Reactions of 8b with CS_2. In the drybox, an NMR tube was charged with 9.8 mg (0.016 mmol) of **8b** in C_6D_6. After fitting the tube with a Cajon adaptor attached to a Kontes vacuum stopcock, it was attached to a vacuum line equipped with an MKS Baratron gauge. CS_2 (0.078 mmol, 5 equiv) was condensed in at −196 °C, and the tube flame sealed under vacuum. Upon thawing, the carbonate precipitated out of solution. Brief heating at 46 °C was necessary to dissolve the compound. After standing for 2 h at room temperature, ^1H NMR analysis showed two methoxide resonances at δ 4.56 (**9b**) and 3.54 (**8b**) in a ~1:7 ratio. After standing overnight at room temperature, similar NMR analysis showed growth of the downfield methoxide resonance, now in a ~1:3 ratio. Complete conversion to **9b** was observed after 5 days at room temperature. The yield of **9b** was 88% by integration against the C_6D_5H resonance.

Re-formation of 2b from 8b. In the drybox, a 100-mL Schlenk flask was charged with 30 mg (0.048 mmol) of $(CO)_3$(diars)ReO(CO)OCH_3 and 20 mL of toluene. The flask was removed from the box and attached to a Schlenk line. A suba seal was placed in the neck of the flask, and N_2 gas admitted through a 22-gauge needle. The flask was vented with a 24-gauge needle placed next to the N_2 inlet. N_2 gas was bubbled through the solution. After 2 days, 10 mL of toluene was added via syringe to compensate for evaporation. After 5 days, the toluene was removed in vacuo, and the flask taken into the drybox. The pale yellow residue dissolved in 4 mL of benzene and filtered through a plug of Celite. The benzene was removed to yield 19 mg (0.033 mmol, 70%) of the methoxide complex **2b**. ^1H NMR (C_6D_6) δ 7.01 (m, 4 H, diars-C*H*), 4.28 (s, 3 H, OCH_3), 1.29 (s, 6 H, diars-CH_3), 1.12 (s, 6 H, diars-CH_3). Lit.:[40] ^1H NMR (C_6D_6) δ 7.01 (m, 4 H, diars-C*H*), 4.29 (s, 3 H, OCH_3), 1.29 (s, 6 H, diars-CH_3), 1.12 (s, 6 H, diars-CH_3).

Acknowledgment. We are grateful for financial support of this work from National Institutes of Health Grant No. GM-25451. R.D.S. expresses his gratitude for a Squibb Fellowship (1990–91). We wish to thank Dr. Milton Orchin for his willingness to exchange unpublished information about analogous results obtained independently in his laboratory during the course of this work.

Supplementary Material Available: Tables of positional parameters, anisotropic thermal parameters, and root-mean-amplitudes of **11b** (8 pages). Ordering information is given on any current masthead page.

OM920326J

Hydrodimetalation of Alkynes and Diynes: Diiron Complexes of μ-η^1:η^2-Alkenyl Ligands with Pendant Alkynes: Crystal and Molecular Structure of $Fe_2(CO)_6(\mu\text{-}PPh_2)(\mu_2\text{-}\eta^1\text{:}\eta^2\text{-}CH{=}CH_2)$ and $Fe_2(CO)_6(\mu\text{-}PPh_2)(\mu_2\text{-}\eta^1\text{:}\eta^2\text{-}C(C{\equiv}CMe){=}CHMe)$

Shane A. MacLaughlin, Simon Doherty, Nicholas J. Taylor, and Arthur J. Carty*

Guelph-Waterloo Centre for Graduate Work in Chemistry, Waterloo Campus, Department of Chemistry, University of Waterloo, Waterloo, Ontario, Canada N2L-3G1

Received June 2, 1992

The reactions of alkynes and diynes with $HFe_2(CO)_7(\mu\text{-}PPh_2)$ gives the bridging alkenyl complexes $Fe_2(CO)_6(\mu\text{-}PPh_2)(\mu\text{-}\eta^1\text{:}\eta^2\text{-}R^2C{=}CHR^1)$. In the case of alkynes $R^1C{\equiv}CR^2$ (R^2 = TMS, H, Ph, OEt, CH_2Cl, and R^1 = H, or R^2 = R^1 = Ph) hydrodimetalation affords a single major isomer in which the stereochemistry of the substituents on the original unsaturated organic substrate is cis. There is also a high regiospecificity of reaction leading to gem dihydrides in the final products. The X-ray structure of the parent vinyl complex $Fe_2(CO)_6(\mu\text{-}PPh_2)(\mu_2\text{-}\eta^1\text{:}\eta^2\text{-}CH{=}CH_2)$ (**5**) has been determined. Crystals of **5** are monoclinic, space group $P2_1/c$, with a = 14.695 (4) Å, b = 11.410 (2) Å, c = 12.163 (3) Å, β = 92.90 (2) Å, V = 2037.5 (8) Å^3, and Z = 4. Refinement converged at R = 0.028 and R_w = 0.027 on the basis of 2902 observed reflections. A similar procedure was used to prepare the first diiron alkenyl complexes $Fe_2(CO)_6(\mu\text{-}PPh_2)(\mu\text{-}\eta^1\text{:}\eta^2\text{-}R^2C{=}CHR^1)$ [R^1 = Ph, H, Me and R^2 = C≡CPh, $C_6H_4C{\equiv}CH$, C≡CMe] containing the pendant unsaturated functionalities, C≡CR. The structure of $Fe_2(CO)_6(\mu\text{-}PPh_2)(\mu\text{-}\eta^1\text{:}\eta^2\text{-}C(C{\equiv}CMe){=}CHMe)$ has been determined by single-crystal X-ray diffraction studies. This compound crystallises in the monoclinic space group $P2_1/n$ with a = 10.966 (2) Å, b = 13.082 (3) Å, c = 16.180 (2) Å, β = 90.35 (1)°, V = 2320.6 (8) Å^3, and Z = 4. Refinement converged at R = 0.028 and R_w = 0.033 on the basis of 4397 observed reflections. The molecule $Fe_2(CO)_6(\mu\text{-}PPh_2)(\mu\text{-}\eta^1\text{:}\eta^2\text{-}C(C{\equiv}CMe){=}CHMe)$ contains an yne–enyl ligand resulting from regiospecific hydrodimetalation at the diyne substrate (MeC≡CC≡CMe). In the major isomer the pendant unsaturated moiety is found on C_α. The variable temperature $^{13}C\{^1H\}$ NMR spectra of **5** revealed dynamic behavior involving three independent processes: two low-energy trigonal rotations of vastly disparate energies, and a much higher energy process involving equilibration of the two nonequivalent tricarbonyl iron sites.

Introduction

Numerous synthetic approaches exist for the preparation of σ- and σ–π alkenyl complexes including oxidative addition of a C–H bond of an alkene,[1] decarbonylation of an appropriate acyl cluster,[2] protonation of anionic acetylene derivatives,[3] reaction of μ-alkylidyne complexes with diazo compounds[4] or 1,2-disubstituted alkenes,[5] reaction of a

(1) (a) Nubel, P. O.; Brown, T. L. *J. Am. Chem. Soc.* **1982**, *104*, 4955. (b) Nubel, P. O.; Brown, T. L. *J. Am. Chem. Soc.* **1984**, *106*, 644. (c) Franzreb, K. H.; Kreiter, C. G. *J. Organomet. Chem.* **1983**, *246*, 189. (d) Keister, J. B.; Shapley, J. R. *J. Organomet. Chem.* **1975**, *85*, C29.

(2) (a) Seyferth, D.; Hoke, J. B.; Womack, G. B. *Organometallics* **1990**, *9*, 2662. (b) Hoke, J. B.; Dewan, J. C.; Seyferth, D. *Organometallics* **1987**, *6*, 1816.

(3) (a) Yanez, R.; Ros, J.; Mathieu, R.; Solans, X.; Font-Bardia, M. *J. Organomet. Chem.* **1990**, *389*, 319. (b) Seyferth, D.; Hoke, J. B.; Dewan, J. C. *Organometallics* **1987**, *6*, 895.

0276-7333/92/2311-4315$03.00/0

mononuclear σ-alkenyl complex with a corresponding metal carbonyl,[6] and β-hydride abstraction from a μ-alkylidene complex.[7] But by far the most general approach is hydrometalation,[8] namely, the addition of a metal hydride across the unsaturated bond of an organic substrate. Similarily μ-η^1:η^2-enyne complexes can in principle be prepared by the hydrometalation of the triple bond of a diyne.[9] More elaborate procedures have involved facile alkenyl–vinylidene coupling at a single metal center[10] and oxidative coupling of alkenyl ligands.[10j] Recently, Hogarth[10k] has employed a synthetic strategy for the preparation of phosphido-bridged diiron vinyl complexes utilizing diphenylvinylphosphine coordination at iron with subsequent P–C bond cleavage to generate phosphido and ethenyl bridged compounds.

To our knowledge there are no examples of binuclear iron triad metal carbonyls containing coordinated yne–enyl ligands (RC≡CC=CRH) even though such moieties should exhibit synthetic potential for the preparation of higher nuclearity homo- and heterometallic cluster complexes. Interest in such organometallic monomers containing pendant unsaturated groups in conjunction with organic ligands lies in their ability to act as precursors for specialty polymers which may exhibit practical conducting, optical, or mechanical properties.[11]

Complexes possessing coordinated yne–enyl ligands,[10,12] either σ- or σ,π-bound, containing a pendant unsaturated hydrocarbyl unit have previously been reported for a small number of metal complexes including $Ru(CO)_2\{C(C{\equiv}CPh){=}CPhHgCl\}Cl(PMe_2Ph)_2$,[12] $Os(PMe_3)_4(PhC_3CHPh)$,[10i] and $Fe(dmpm)_2(PhC_3CHPh)$,[10g] but very few have been prepared by simple hydrometalation reactions despite the synthetic versatility of this approach. Recently we have shown[13] that the σ,π-acetylide complex $Fe_2(CO)_6(\mu\text{-}PPh_2)(\mu_2\text{-}\eta^1{:}\eta^2\text{-}C{\equiv}CR)$ can be utilized in the synthesis of binuclear complexes bearing four carbon polyunsaturated ligands via the addition of 2 mol equiv of diazomethane at C_α and C_β. We also revealed that these complexes were accessible via hydrometalation reactions with the appropriate unsaturated hydrocarbyl ligand. In this paper we fully explore the synthetic potential of the readily accessible and extremely reactive hydrido phosphido complex $HFe_2(CO)_7(\mu\text{-}PPh_2)$[14] toward alkynes and diynes. The results of this study, which indicate high regio- and stereochemical control of hydrodimetalation, are presented herein.

Results and Discussion

The reactions of bimetallic carbonyl hydrides with acetylenes are well-known, usually proceeding under thermal[15] or photolytic[8a,b] activation and leading to products where the stereochemistry of the original organic substrate is normally cis, although more recently hydrometalation has been recognized to proceed through trans insertion with subsequent isomerization to the thermodynamically more stable cis isomer.[30] We have discovered that reaction of the metal carbonyl hydride $HFe_2(CO)_7(\mu\text{-}PPh_2)$ (1) with diynes generates polyunsaturated, strongly bound hydrocarbyl ligands. Since the hydride can be readily prepared in high yield, this represents a powerful method for synthesising yne–enyl ligands at a binuclear center.

Treatment of a freshly prepared sample of the sodium salt of the dianion $[Fe_2(CO)_8]^{2-}$ with 1 equiv of chlorodiphenylphosphine in THF at 0 °C over 6 h affords crude $[Fe_2(CO)_8(\mu_2\text{-}PPh_2)]^-$ (I), which after workup is obtained

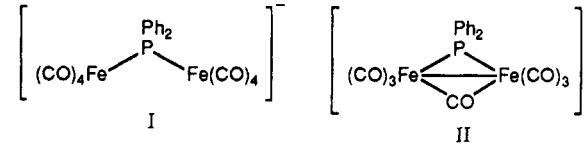

I II

as an orange/yellow air-sensitive powder. Spectroscopic data support a structure with a phosphido ligand bridging an open M–M bond. The ν(CO) IR and $^{13}C\{^1H\}$ NMR data give no indication of the presence of a bridging carbonyl. The $^{31}P\{^1H\}$ chemical shift occurs at a position approxi-

(4) Casey, C. P.; Austin, E. A.; Rheingold, A. L. *Organometallics* **1987**, *6*, 2157.

(5) (a) Casey, C. P.; Gohdes, M. A.; Meszaros, M. W. *Organometallics* **1986**, *5*, 196. (b) Casey, C. P.; Fagan, P. J.; Miles, W. H.; Marder, S. R. *J. Mol. Catal.* **1983**, *21*, 173. (c) Casey, C. P.; Meszaros, M. W.; Colborn, R. E.; Roddick, D. M.; Miles, W. H. Gohdes, M. A. *Organometallics* **1986**, *5*, 1879. (d) Casey, C. P.; Meszaros, M. W.; Fagan, P. J.; Bly, R. K.; Colborn, R. E. *J. Am. Chem. Soc.* **1986**, *108*, 4053. (e) Casey, C. P.; Meszaros, M. W.; Marder, S. R.; Bly, R. K.; Fagan, P. J. *Organometallics* **1986**, *5*, 1873. (f) Casey, C. P.; Fagan, P. J.; Miles, W. H. *J. Am. Chem. Soc.* **1982**, *104*, 1134. (g) Casey, C. P.; Fagan, P. J. *J. Am. Chem. Soc.* **1982**, *104*, 4950. (h) Casey, C. P.; Meszaros, M. W.; Marder, S. R.; Fagan, P. J. *J. Am. Chem. Soc.* **1984**, *106*, 3680. (i) Casey, C. P.; Marder, S. R.; Fagan, P. J. *J. Am. Chem. Soc.* **1983**, *105*, 7197.

(6) (a) Andrianov, V. G.; Struchkov, Y. T. *J. Chem. Soc., Chem. Commun.* **1968**, 1590. (b) Nesmeyanov, A. N.; Rybinskaya, M.; Rybin, L. V.; Kaganovich, V. S.; Petrovskii, P. V. *J. Organomet. Chem.* **1971**, *31*, 257. (c) Ros, J.; Mathieu, R. *Organometallics* **1983**, *2*, 771. (d) Fryzuk, M. D.; Jones, T.; Einstein, F. W. B. *Organometallics* **1984**, *3*, 185.

(7) (a) Casey, C. P.; Konings, M. S.; Gohdes, M. A.; Meszaros, M. W. *Organometallics* **1988**, *7*, 2103. (b) Finnimore, S. R.; Knox, S. A. R.; Taylor, G. E. *J. Chem. Soc., Chem. Commun.* **1980**, 441. (c) Adams, R. D.; Dawoodi, Z.; Foust, D. F. *Organometallics* **1982**, *1*, 411. (d) Casey, C. P.; Marder, S. R.; Adams, B. R. *J. Am. Chem. Soc.* **1985**, *107*, 7700.

(8) (a) Conole, G.; Henrick, K.; McPartlin, M.; Horton, A. D.; Mays, M. J. *New J. Chem.* **1988**, *12*, 559. (b) Horton, A. D.; Kemball, A. C.; Mays, M. J. *J. Chem. Soc., Dalton Trans.* **1988**, 2953. (c) Deeming, A. J.; Hasso, H.; Underhill, M. *J. Chem. Soc., Dalton Trans.* **1975**, 1614. (d) Burgess, K. *Polyhedron* **1984**, *3*, 1175. (e) Romero, A.; Santos.; Lopez, J.; Eschavarren, A. M. *J. Organomet. Chem.* **1990**, *391*, 219. (f) Graff, J. L.; Wrighton, M. S. *J. Am. Chem. Soc.* **1980**, *102*, 2123. (g) Jackson, W. G.; Johnson, B. F. G.; Kelland, J. W.; Lewis, J.; Schorpp, K. T. *J. Organomet. Chem.* **1975**, *87*, C27. (h) Torres, M. R.; Santos, A.; Perales, A.; Ros, J. *J. Organomet. Chem.* **1988**, *353*, 221. (i) Deeming, A. J.; Hasso, S.; Underhill, M. *J. Organomet. Chem.* **1974**, *80*, C53. (j) Chi, Y.; Chen, B. F.; Wang, S. L.; Chiang, R. K.; Hwang, L. S. *J. Organomet. Chem.* **1989**, *377*, C59. (l) Yanez, R.; Ros, J.; Mathieu, R. *J. Organomet. Chem.* **1990**, *389*, 197. (m) Torres, M. R.; Vegas, A.; Santos, A.; Ros, J. *J. Organomet. Chem.* **1986**, *309*, 169.

(9) (a) Jia, G.; Gallucci, J. C.; Rheingold, A. L.; Haggerty, B. S.; Meek, D. W. *Organometallics* **1991**, *10*, 3459. (b) Alcock, N. M.; Hill, A. F.; Melling, R. P. *Organometallics* **1991**, *10*, 3898. (c) Harris, M. J. C.; Hill, A. F. *Organometallics* **1991**, *10*, 3903.

(10) (a) McMullen, A. K.; Selegue, J. P.; Wang, J. G. *Organometallics* **1991**, *10*, 3421. (b) Dobson, A.; Moore, D. S.; Dobinson, S. D.; Hursthouse, M. D.; New, J. *Polyhedron* **1985**, *4*, 1119. (c) Wakatsuki, Y.; Yamazaki, H.; Kumegawa, N.; Satoh, T.; Satoh, J. Y. *J. Am. Chem. Soc.* **1991**, *113*, 9604. (d) Jia, G.; Meek, D. W. *Organometallics* **1991**, *10*, 1444. (e) Jia, G.; Rheingold, A. L.; Meek, D. W. *Organometallics* **1989**, *8*, 1378. (f) Field, L. D.; George, A. V.; Hambley, T. W. *Inorg. Chem.* **1990**, *29*, 4565. (g) Hills, A.; Hughes, D. L.; Jimenez-Tenorio, M.; Leigh, G. J.; McGeary, C. A.; Rowley, A. T.; Bravo, M.; McKenna, C. E.; McKenna, M. C. *J. Chem. Soc., Chem. Commun.* **1991**, 522. (h) Moran, G.; Green, M.; Orpen, A. G. *J. Organomet. Chem.* **1983**, *250*, C15. (i) Field, L. D.; George, A. V.; Malouf, E. Y.; Slip, I. H. M.; Hambley, T. W. *Organometallics* **1991**, *10*, 3842. (j) Goting, J.; Otto, H.; Werner, H. *J. Organomet. Chem.* **1985**, *287*, 247. (k) Hogarth, G. *J. Organomet. Chem.* **1991**, *407*, 91.

(11) (a) Bandy, J. A.; Bunting, H. E.; Garcia, M-H.; Green, M. L. H.; Marder, S. R.; Thompson, M. E.; Bloor, D.; Kolinsky, P. V.; Jones, R. J.; Perry, J. W. *Polyhedron* **1992**, *11*, 1429. (b) *Metal Containing Polymer Systems*; Sheats, J. E., Carraher, C. E., Jr.; Pittman, C. U., Jr., Eds.; Plenum Press: New York, 1985. (c) *Inorganic and Organometallic Polymers*; Zeldin, M., Wynne, K. J., Allcock, H. R., Eds.; ACS Symposium Series No. 360; American Chemical Society: Washington, DC, 1988. (d) *Organometallic Polymers*; Carraher, C. E., Sheats, J. E., Jr., Pittman, C. U., Jr., Eds.; Academic Press: New York, 1978.

(12) Dauter, Z.; Mawby, R. J.; Reynold, C. D.; Saunders, D. R. *J. Chem. Soc., Dalton Trans.* **1986**, 433.

(13) Breckenridge, S. M.; MacLaughlin, S. A.; Taylor, N. J.; Carty, A. J. *J. Chem. Soc., Chem. Commun.* **1991**, 1718.

(14) (a) Osterloh, W. T. Ph.D. Thesis, University of Texas, Austin, TX, 1982. (b) Baker, R. T.; Calabrese, J. C.; Krusig, P. J.; Therien, M. J.; Trogler, W. C. *J. Am. Chem. Soc.* **1988**, *110*, 8392.

(15) Lourdichi, M.; Mathieu, R. *Organometallics* **1986**, *5*, 2067.

mately 75 ppm to high field of the range typical for $Fe_2(\mu\text{-}PPh_2)$ complexes containing a metal–metal interaction.[16a] Salts of I readily decarbonylate in solution or slowly in the solid state on exposure to light, yielding quantitatively the heptacarbonyl anion II, the structure of which has been determined by a single-crystal X-ray diffraction study of its tetraethylammonium salt.[14a] Chemically I and II behave similarly, protonation resulting in the evolution of CO and the generation of the extremely air-sensitive and reactive hydride complex $HFe_2(CO)_7(\mu\text{-}PPh_2)$ (1). Attempts to isolate 1 as a crystalline solid were unsuccessful. However, in situ generation of 1 prior to reaction with alkynes proved adequate for the preparation of the η^2-alkenyl complexes. The spectroscopic properties of 1 are consistent with a structure containing a phosphido ligand bridging a metal–metal interaction. The $^{31}P\{^1H\}$ chemical shift of the phosphido bridge [δ = 170.4] appears approximately 120 ppm to low field of that in I, consistent with the presence of a metal–metal bonding interaction.[16a] The presence of the hydride ligand was confirmed by the observation of a single high-field resonance in the ^1H NMR spectrum (δ = −9.98 ppm, $^2J_{PH}$ = 53.9 Hz). Although the magnitude of $^2J_{PH}$ may be indicative of a phosphido–hydrido bridging arrangement,[16b,c] the presence of a terminal hydride cannot be ruled out.

On addition of alkynes and the diynes PhC≡CC≡CPh, MeC≡CC≡CMe, and HC≡CC_6H_4C≡CH to a solution of $HFe_2(CO)_7(\mu\text{-}PPh_2)$, a brisk gas evolution was observed, slowing gradually over the course of the reaction. The progress of the reaction was measured by monitoring the ν(CO) IR bands assignable to the starting material. In all cases the final reaction solution was orange-red. Without exception a single major product was observed, although for R = TMS, Ph, C_6H_4(C≡CH) a second product assignable as a minor isomer resulting from the opposite regiospecificity of insertion was also found to be present, albeit in very small quantities. The $\mu\text{-}\eta^1\text{:}\eta^2$-alkenyl complexes 2–11 were obtained as crystalline materials, stable both in solution and in the solid state. They were identified by microanalysis and ^1H and $^{13}C\{^1H\}$ NMR spectroscopy and in the case of 5 and 10 by single-crystal X-ray structural analyses.

Seyferth has recently described the use of the anion $[Fe_2(CO)_6(\mu\text{-}PPh_2)]^-$ (III) in the preparation of complexes of the type $Fe_2(CO)_6(\mu\text{-}PPh_2)(\mu\text{-E})$ (E = SR, PR_2, NR_2CS, RSCS, CH=CH_2).[17] Electronically unsaturated III is a useful reagent for the synthesis of these doubly bridged complexes notably $Fe_2(CO)_6(\mu\text{-}PPh_2)(\mu_2\text{-}\eta^1\text{:}\eta^2\text{-CH=CH}_2)$ via reaction with acryloyl chloride affording an acyl-bridged intermediate and subsequently the alkenyl complex by decarbonylation.

The structural characterization of σ–π-alkenyl complexes, particularly the stereochemical relationships between the various substituents, rests heavily on ^1H and ^{13}C NMR spectroscopy. With an extensive array of alkenyl complexes in the literature the correlation of ^1H and ^{13}C NMR parameters often provides an unambiguous proof of stereochemistry.[18,19] Statistically the hydrodimetalation of an unsymmetrical terminal alkyne (RC≡CH) would be expected to afford three possible isomers,[18] a, b, and c.

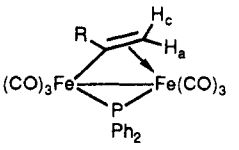

a

α-metalated, *cis* adddition

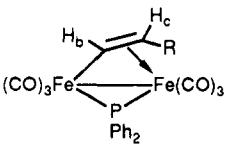

b

β-metalated, *trans* adddition

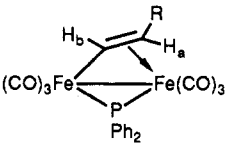

c

β-metalated, *cis* adddition

Isomers a and c are the α- and β-metalated products arising from the cis addition of $[Fe_2]$–H across the alkyne triple bond, whereas b represents the products from trans addition. The cis and trans addition products are indistinguishable for α-metalation in the absence of deuterium-labeling experiments. We find no evidence for isomers of type b in this work strongly suggesting that the stereochemistry of $[Fe_2]$–H addition to cis. This result is consistent with a number of other observations of cis-hydrometalation chemistry in binuclear systems including $Mn_2(\mu\text{-H})(\mu\text{-}PPh_2)(CO)_8$,[8a] $Re_2(\mu\text{-H})_2(CO)_8(\mu\text{-dppm})$, and $[NEt_3H][Fe_2(CO)_6(\mu\text{-CO})(\mu\text{-}PPh_2)(\mu\text{-S}^t\text{Bu})]$.[2a]

In the present case the addition of the $[Fe_2]$–H group across the triple bond of the unsaturated substrate also proved to be highly regioselective, favoring isomer a formed from Markovnikov type addition, i.e., α-metalation. Relevant ^1H and ^{13}C NMR data for all of the compounds characterised are given in Tables I and II, respectively.

The protons attached to the σ–π-vinyl ligand resonate at chemical shifts[2a] vastly different from those associated with normal olefinic protons.[21] Thus the resonance assignable to H_b, the proton attached to the σ bound C_α of the alkenyl ligand, is observed downfield (δ 8.3–9.0 ppm), while the remaining proton H_c (H_a and H_c for HC≡CH hydrodimetalation) is located at high field (δ 1.46–4.29 ppm). A typical spectrum showing these features is illustrated in Figure 1. These high- and low-field shifts of the alkenyl protons are a consequence of the reduced bond order of the alkenyl double bond resulting from π-coordination and shielding of the proton(s) on the β-carbon atom by the metal atom to which C_β is π-coordinated.

The ^{13}C NMR chemical shifts of the carbon atoms (C_α and C_β) of complexes 2–11 are, like the corresponding ^1H NMR spectra, characteristic of $\mu\text{-}\eta^1\text{:}\eta^2$-alkenyl ligands

(16) (a) Carty, A. J.; MacLaughlin, S. A.; Nucciarone, D. *Phosphorus-31 NMR Spectroscopy in Stereochemical Analysis: Organic Compounds and Metal Complexes*; Verkade, J. G., Quinn, L. D., Eds.; VCH Publishers: New York, 1987; Chapter 16, p 605. (b) Patel, V. D.; Cherkas, A. A.; Nucciarone, D.; Taylor, N. J.; Carty, A. J. *Organometallics* **1985**, *4*, 1792. (c) Walther, B.; Hartung, H.; Bottcher, H.-C.; Baumeister, U.; Bohland, U.; Reinhold, J.; Sieler, J.; Ladriere, J.; Schiebel, H.-M. *Polyhedron* **1991**, *10*, 2423.

(17) Seyferth, D.; Brewer, K. S.; Wood, T. G.; Cowie, M.; Hilts, R. W. *Organometallics* **1992**, *11*, 2570.

(18) Van der Zeijden, A. A. H.; Bosch, W. H.; Berke, H. *Organometallics* **1992**, *11*, 563.

(19) (a) Ros, J.; Vinas, J. M.; Mathieu, R.; Solans, X.; Font-Bardia, M. *J. Chem. Soc., Dalton Trans.* **1988**, 281. (b) King, R. B.; Treichel, P. M.; Stone, F. G. A. *J. Am. Chem. Soc.* **1961**, *83*, 3600. (c) Casey, C. P.; Marder, S. R.; Colborn, R. E.; Goodson, P. A. *Organometallics* **1986**, *5*, 199. (d) Nubel, P. O.; Brown, T. L. *J. Am. Chem. Soc.* **1984**, *106*, 3475. (e) Grevels, F. W.; Schulz, D.; Von Gustorf, E. K.; Bunbury, D. St. P. *J. Organomet. Chem.* **1975**, *91*, 341. (f) Torres, M. R.; Santos, A.; Ros, J.; Solans, X. *Organometallics* **1987**, *6*, 1091. (g) Romero, A.; Santos, A.; Vegas, A. *Organometallics* **1988**, *7*, 1988. (h) Herberich, G. H.; Barlage, W. *Organometallics* **1987**, *6*, 1924. (i) Chisholm, M. H.; Clark, H. C.; Manzer, L. E. *Inorg. Chem.* **1972**, *11*, 1279. (j) Bottrill, M.; Green, M. *J. Am. Chem. Soc.* **1977**, *99*, 5795.

(20) (a) Seyferth, D.; Archer, C. M.; Ruschke, D. P.; Cowie, M.; Hilts, R. W. *Organometallics* **1991**, *10*, 3363. (b) Aime, S.; Milone, C.; Sappa, E.; Tiripicchio, A.; Tiripicchio-Camellini, M. *J. Chem. Soc., Dalton Trans.* **1979**, 1155. (c) Hickey, J. P.; Huffman, J. C.; Todd, J. L. *Inorg. Chim. Acta* **1978**, *28*, 77.

(21) *Spectroscopic Determination of Organic Compounds*; Silverstein, R. M., Bassler, G. C., Morrill, T. C., Eds.; Wiley: New York, 1981.

Table I. ^{1}H NMR Spectral Data for the μ-η^1:η^2-Vinyl Complexes 2–11

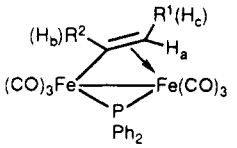

complex	R^1	R^2	$\delta(H_a)$	$\delta(H_b)$	$\delta(H_c)$	J_{HaHb}/Hz	J_{HaHc}/Hz	J_{HbHc}/Hz
2a	H	TMS	2.70		3.39		3.7	
2b	TMs	H	2.64	8.62		14.9		
3a	H	Ph	2.21		2.99		3.0	
3b	Ph	H	4.29	8.93		13.4		
4a	H	$C_6H_4(C_2Ph)$	2.22		2.98		3.1	
4b	$C_6H_4(C_2Ph)$	H	3.88	8.76		13.6		
5	H	H	2.43	8.32	3.32	13.4	2.1	9.6
6	Ph	Ph	3.75					
7	H	CH_2Cl	2.19		3.26		3.4	
8	H	OEt	1.46		2.77		5.7	
9	H	$CMe{=}CH_2$	2.02		2.70		3.7	
10	Me	$C{\equiv}CMe$	2.87					
11	Ph	$C{\equiv}CPh$	3.59					

Table II. $^{13}C\{^1H\}$ NMR Spectral Data for C_α and C_β for the μ-η^1:η^2-Vinyl Complexes 2–11

complex	R^1	R^2	$\delta(C_\alpha)$	J(PC)/Hz	$\delta(C_\beta)$	J(PC)/Hz
2a	H	TMS	187.87	25.2	75.25	17.1
2b	TMS	H	164.23	26.4	88.61	12.3
3a	H	Ph	189.04	20.1	66.19	13.3
3b	Ph	H	145.74	27.1	93.57	17.5
4a	H	$C_6H_4C{\equiv}CH$	186.93	19.9	66.18	13.4
4b	$C_6H_4C{\equiv}CH$	H				
5	H	H	158.78	26.9	72.47	15.3
6	Ph	Ph	181.27	19.5	85.36	17.5
7	H	CH_2Cl	178.06	21.4	70.56	13.6
8	H	OEt	220.30	20.2	47.96	8.9
9	H	$MeC{=}CH$	194.33	20.6	63.23	13.5
10	Me	$C{\equiv}CMe$	153.02	24.5	86.82	15.3
11	Ph	$C{\equiv}CPh$	144.57	23.4	89.99	17.0

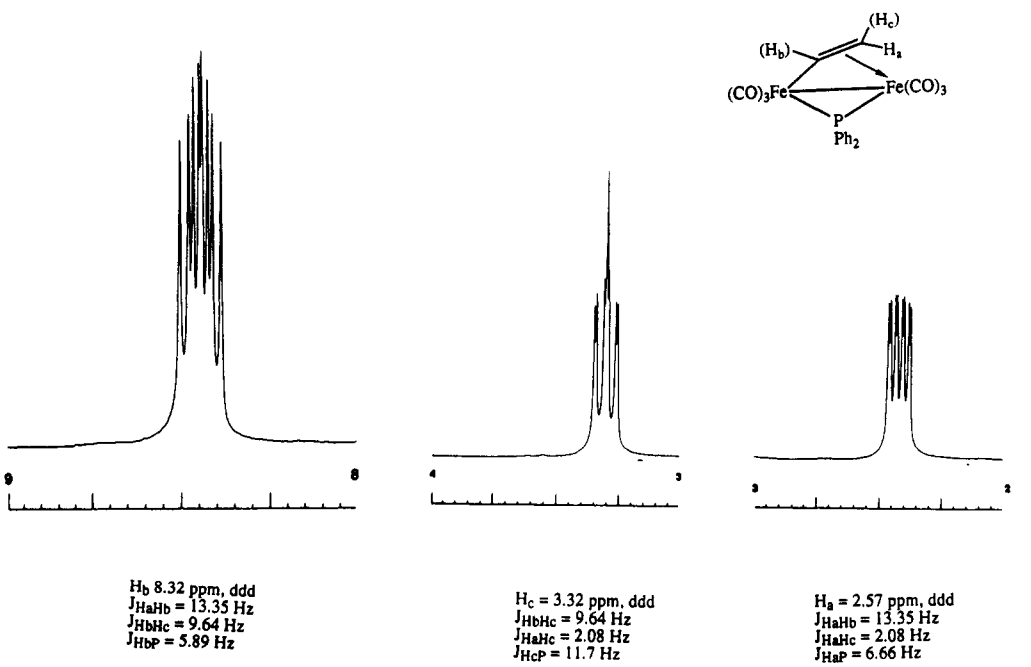

Figure 1. ^{1}H NMR spectra of $Fe_2(CO)_6(\mu\text{-}PPh_2)(\mu_2\text{-}\eta^1\text{:}\eta^2\text{-}CH{=}CH_2)$ (250 MHz, $CDCl_3$).

(Table II). The chemical shifts of C_α and C_β do not appear in the region normally associated with olefinic carbon atoms.[21] The values of $\delta(C_\alpha)$ and $\delta(C_\beta)$ for compounds **5**–**11** compare well with the values recently reported for the related μ-σ-π vinyl complexes $Fe_2(CO)_6(\mu\text{-}SR)(\mu\text{-}CR^1{=}CR^2R^3)$.[20a] Thus C_α appears to be shifted downfield (δ 144–220 ppm) as a result of a contribution from the carbene type resonance structure B while the signals associated with C_β are shifted upfield (in the range 38–93 ppm) as a consequence of the metallocyclic resonance contribution of B imparting a degree of sp^3 like character to C_β.

Although the symmetrical alkynes PhCCPh and HCCH gave only single products, for the vast majority of unsymmetrical alkynes employed here cis addition should lead to two isomeric forms, corresponding to the two possible

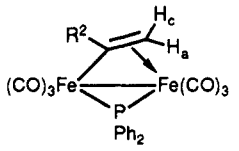

A

σ,π vinyl contribution

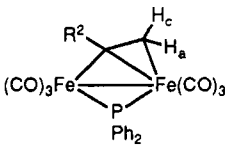

B

metallocyclic/carbene resonance contribution

modes of insertion into the [Fe]-H bond, α- and β-metalation,[18] a and c. Structural assignments for these isomeric forms have been inferred from ^{1}H NMR spectroscopic data. Where isomeric products were formed they were differentiated on the basis of their $^2J_{H-H}$ and $^3J_{H-H}$ coupling constants (Table I), although the abnormal chemical shifts of these vinylic protons were enough to assign the regiochemistry of insertion assuming that cis addition had occurred. For **2a** and **3a** the observation of two high-field vinylic signals (δ = 2.70, 3.39 and δ 2.21, 2.99 ppm, respectively) with a small geminal coupling constants ($^2J_{HH}$ = 3.69 and 2.98 Hz, respectively) indicated a terminal olefin. For their corresponding isomers **2b** and **3b** a low-field signal (H_b, δ = 8.62 and 8.93 ppm, respectively) and a high-field resonance (H_a, δ = 2.64 and 4.29, respectively) with larger vicinal coupling constants ($^3J_{HH}$ = 14.91 and 13.40 Hz, respectively) was indicative of an E-metalated olefin. These values are very close to the cis and trans coupling constants observed in uncoordinated olefins. Additional evidence for these assignments was provided by an examination of the ^{1}H-coupled ^{13}C NMR spectra for **2a** and **3a**. One of the vinylic carbon atoms appears as a doublet of doublets of doublets at δ 75.25 (C_β) and a $^2J_{CP}$ coupling constant of 17.11 Hz and $^1J_{CH}$ couplings of 154.90 and 152.0 Hz. The other vinylic carbon at δ 187.87 appears as a doublet with $^2J_{CP}$ = 25.16 Hz. Similar couplings for $^1J_{CH}$ and $^2J_{CP}$ were observed in **3a**, and these data unambiguously prove that isomer a is the correct structure for **2a** and **3a**. The ^{1}H-coupled ^{13}C NMR spectra of their minor isomeric counterparts **2b** and **3b** also exhibit two vinylic carbon resonances. For instance, these signals appear at high field (δ = 88.61) as a doublet of doublets with $^1J_{CH}$ = 160.95 Hz and $^2J_{PC}$ = 12.25 Hz for C_β, while C_α appears at δ 164.23 with a similar multiplicity ($^1J_{CH}$ = 148.27 Hz and $^2J_{PC}$ = 26.35 Hz) in **3b**. Thus examination of the ^{1}H and ^{13}C ^{1}H-coupled NMR spectra readily provide enough information to distinguish between the α- and β-metalated products. In previous studies an increasing proportion of the isomer with the alkyl substituent on the α carbon of the vinyl ligand has been attributed to the increasing steric bulk of the alkyl group, thereby favoring the less crowded site on the vinyl carbon atom, a trend similar to that observed here. Although the formation of complexes **2–10** can be fully accounted for on the basis of cis addition of [Fe_2]–H across the alkyne triple bond it is worth noting that cis and trans addition have been observed in other binuclear systems. In the latter cases it has been suggested that the cis/trans stereochemistry shows a delicate balance between various factors including steric effects, identity of the metal, oxidation state, auxilliary ligands and the electronic nature of the substituent on the alkyne.[8a]

In the corresponding reaction of **1** with the diynes PhC≡CC≡CPh, MeC≡CC≡CMe, and HC≡CC_6H_4C≡CH, μ-σ,π-vinyl complexes **4a**, **4b**, **10**, and **11** analogous to those already discussed were found. ^{1}H NMR spectral data for these compounds confirmed that the molecules are alkenyl complexes containing uncoordinated alkynyl substituents. Only a single isomer was observed in the reactions with 1,4-diphenylbutadiyne and 2,4-hexadiyne, indicating total regiospecificity of insertion, while a minor amount (<5%) of a second isomer was present in the reaction mixture from HC≡CC_6H_4C≡CH and **1**.

The structure of **11** is believed to be similar to that of the major isomer **3a** (eq 1) based on the correspondence of its ^{13}C NMR spectral data in the aromatic region with that of **3b** where the phenyl group is bound to the β carbon atom of the alkenyl bridge. Ipso carbon atoms of phenyl

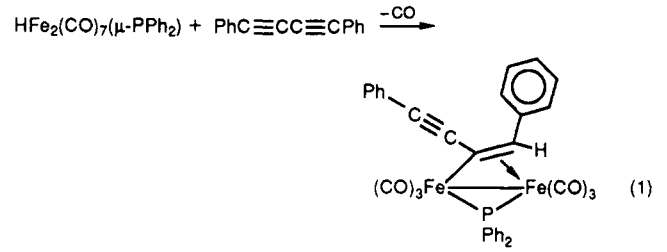

rings attached to C_α appear at low field (δ = 154–157 ppm) of the region normally associated with these carbon resonances and couple to the phosphorus atom of the phosphido bridge with a coupling constant typically less than 3 Hz [e.g., δ = 154.21 ppm, J_{C_i-P} = 2.0 Hz for **6** and δ = 157.17, J_{C_i-P} < 2 Hz for **3a** and δ 157.08, J_{C_i-P} = 2.15 Hz for **4a**). Conversely C_{ipso} of an aromatic ring attached to C_β appears at higher field and couples to the same phosphorus atom more strongly (5 Hz < J_{C_i-P} < 7 Hz). Supporting data include δ = 140.81, J_{C_i-P} = 5.7 Hz for **6** and δ = 140.64, J_{C_i-P} = 5.5 Hz for **3b**. The close agreement between the coupling constants for the ipso carbon of the phenyl ring and the phosphorus atom of the bridging phosphido group (J_{C_i-P}) [δ C_{ipso} = 141.29 ppm, $^4J_{C_i-P}$ = 5.17 Hz for **11**] for **11** and **3b** leaves no doubt as to the regiospecificity of the reaction, i.e., the phenyl group in **11** must also be bound directly to C_β.

^{13}C{^{1}H} NMR spectral data for each of compounds **4a**, **4b**, **10**, and **11** also showed resonances typical of μ-η^1:η^2-vinyl ligands[8a] (Table II) as well as signals characteristic of a free alkynyl group (Figure 6). In **10** and **11** the pendant acetylenic carbon atoms exhibit resonances that are shifted downfield (90–100 ppm) in comparison with organic enynes[22] and η^1-(2-alkynyl)alkenyl complexes (80–90 ppm).[23] A similar and equally unusual effect has been observed in η^1-(1-alkynyl)alkenyl[12] complexes and alkynyl carbenes[24] and may be indicative of the effects of conjugation of the triple bond with the α-carbon of the alkenyl group.

Since the original discovery of fluxionality in μ-σ-π-bound alkenyl ligands by Shapley and co-workers[25a] many examples of dynamic interchange involving binuclear and polynuclear alkenyl and alkynyl complexes have been reported.[20,25] We have previously described the dynamics of exchange in the closely related compounds $M_2(CO)_6$(μ-

(22) Mitsudo, T.; Nakagawa, T.; Watanabe, K.; Hori, Y.; Misawa, H.; Watanabe, Y. *J. Org. Chem.* **1985**, *50*, 565.

(23) (a) Reger, D. L.; Belmore, K. A. *Organometallics* **1985**, *4*, 305. (b) Reger, D. L.; Belmore, K. A.; Mintz, E.; McElligott, P. J. *Organometallics* **1984**, *3*, 134.

(24) Dotz, K. H.; Kuhn, W. *J. Organomet. Chem.* **1985**, *286*, C23.

(25) (a) Shapley, J. R.; Richter, S.; Tachikawa, M.; Keister, J. B. *J. Organomet. Chem.* **1975**, *94*, C43. (b) Dyke, A. F.; Knox, S. A. R.; Naish, P. J.; Taylor, G. E. *J. Chem. Soc., Chem. Commun.* **1980**, 409. (c) Deeming, A. J.; Kimber, R. E.; Underhill, M. *J. Chem. Soc., Dalton Trans.* **1973**, 2589. (d) Lee, K.-W.; Brown, T. L. *Organometallics* **1985**, *4*, 1030. (e) Xue, Z.; Sieber, W. J.; Knobler, C. B.; Kaesz, H. B. *J. Am. Chem. Soc.* **1990**, *112*, 1825. (f) Lee, K.-W.; Pennington, W. T.; Cordes, A. W.; Brown, T. L. *J. Am. Chem. Soc.* **1985**, *107*, 631. (g) Mercer, R. J.; Green, M.; Orpen, A. G. *J. Chem. Soc., Chem. Commun.* **1986**, 567. (h) Ten Hoedt, R. W. M.; Van Koten, G.; Noltes, J. G. *J. Organomet. Chem.* **1977**, *133*, 113. (i) Ten Hoedt, R. W. M.; Noltes, J. G.; Van Koten, G.; Spek, A. L. *J. Chem. Soc., Dalton Trans.* **1978**, 1800. (j) Dyke, A. F.; Knox, S. A. R.; Morris, M. J.; Naish, P. J. *J. Chem. Soc., Dalton Trans.* **1983**, 1417.

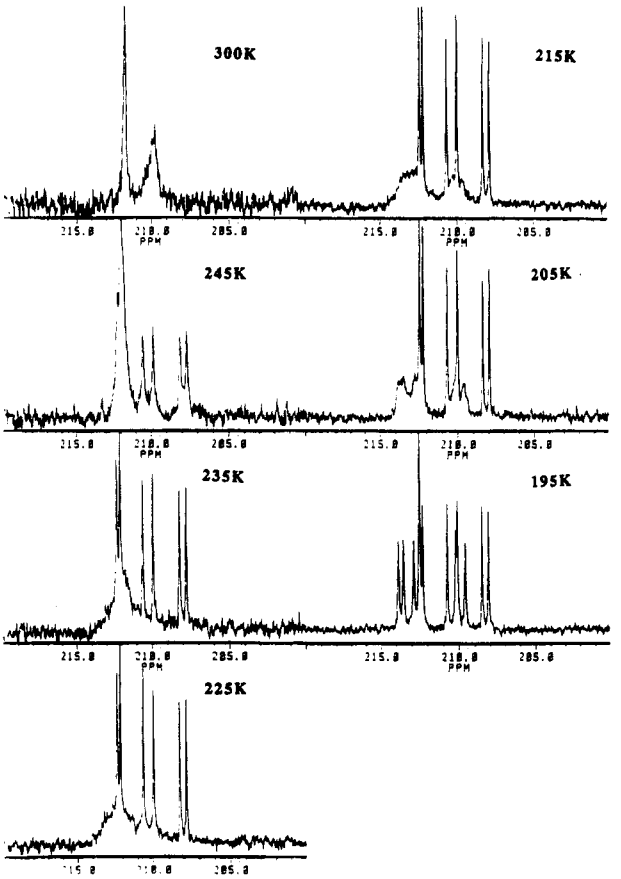

Figure 2. Variable-temperature $^{13}C\{^1H\}$ NMR spectra of the complex $Fe_2(CO)_6(\mu\text{-}PPh_2)(\mu_2\text{-}\eta^1\text{:}\eta^2\text{-}CH{=}CH_2)$.

$PPh_2)(\mu\text{-}\eta^1\text{:}\eta^2\text{-}C{\equiv}CR)$ (M = Fe, Ru, Os)[26] and Seyferth has shown that the μ-sulfido, μ-alkenyl complexes $Fe_2(CO)_6(\mu\text{-}SEt)(\mu\text{-}\eta^1\text{:}\eta^2\text{-}(R)C{=}CH_2)$[20a] are fluxional at ambient temperatures. Similar observations have been made recently for the binuclear complex $Re_2(CO)_7(PPh_3)(\mu\text{-}H)(\mu\text{-}\eta^1\text{:}\eta^2\text{-}CH{=}CH_2)$.[19d] Variable-temperature $^{13}C\{^1H\}$ NMR spectra of $Fe_2(CO)_6(\mu\text{-}PPh_2)(\mu\text{-}\eta^1\text{:}\eta^2\text{-}CH{=}CH_2)$ are shown in Figure 2. Clearly the low-temperature limiting spectrum of **5** (195 K) is in agreement with the solid-state structure, containing six nonequivalent ^{13}CO resonances. At 300 K the $^{13}C\{^1H\}$ NMR spectrum of **5** displays two distinct carbonyl resonances, one relatively sharp the other much broader ($\Delta\nu_{1/2}$ = 150 Hz). Structure d illustrates the

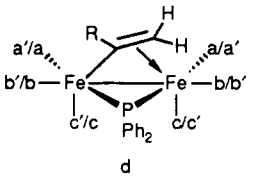

d

	J_{PC}, Hz
a	33
a'	30
b	21
b'	17
c	11
c'	17

three pairs of nonequivalent carbonyl ligands. In the absence of trigonal rotation, the six carbonyl ligands of **5** can be divided into three pairs of ligands with respect to their positions relative to the phosphido bridge, i.e., those trans to the phosphido bridge CO_a, those equatorial and cis CO_b, and the pair of carbonyls axial and cis CO_c to the bridge. It has been shown that the two-bond phosphorus–carbon coupling constant $^2J_{^{31}P\text{-}^{13}CO}$ exhibits a Karplus like relationship to the P–M–C angle, pasing through a sign inversion at ~107° a minimum value at ~90° and reaching a maximum positive value at 180°. Thus on the basis of the P–Fe–C angles in **5**, the coupling constants should decrease in the order $J_{P\text{-}Ca} > J_{P\text{-}Cb} > J_{P\text{-}Cc}$. The values of $^2J_{P\text{-}C}$ extracted from the low-temperature limiting spectrum are consistent with these expectations.[29] The slightly disparate values of $^2J_{PC}$ for pairs of carbonyl ligands on adjacent iron centers reflects the twisting of the carbonyl away from the ideal eclipsed orientation to afford slightly different PMC bond angles.

Although the low temperature $^{13}C\{^1H\}$ spectrum (T = 195 K) has been interpreted as two sets of three carbonyl resonances an unequivocal assignment of the two individual sets abc, and a'b'c' to either Fe(1) or Fe(2) is not possible. Raising the temperature results in the broadening and collapse of one set of three carbonyl resonances (δ = 213.6, 212.7, 209.8), the other set remaining sharp (δ = 212.4, 210.4, 208.3). At 225 K one broad resonance and three sharp doublet resonances remain, allowing an unambiguous assignment for each set of three carbonyl resonances and indicating different barriers to trigonal rotation for the σ- and π-bound $Fe(CO)_3$ units. In the temperature range 225–300 K the broad averaged resonance at δ 211 ppm sharpens, while the three doublet resonances are only starting to undergo exchange. Even at room temperature there is no evidence for the exchange of carbonyls CO_a, CO_b, CO_c with $CO_{a'}$, $CO_{b'}$, and $CO_{c'}$. Qualitatively these spectral characteristics define two fluxional processes: a low-energy trigonal rotation equilibrating three carbonyl ligands followed by a similar higher energy process occurring in the temperature range 245–300 K. Even at room temperature the two iron sites within **5** remain distinct, reflecting the rigid nature of the σ,π-bound hydrocarbyl bridging ligand. A similar broadening of a single set of CO resonances at one metal site followed by exchange of those on the adjacent metal only at much higher temperatures has been reported for the σ–π-allenyl complexes $Ru_2(CO)_6(\mu\text{-}PPh_2)(\mu_2\text{-}\eta^1\text{:}\eta^2\text{-}PhC{=}C{=}CR_2)$.[27a] This nondegeneracy of trigonal rotation at two metal centers, one σ-bound, the other π-bound to a hydrocarbyl ligand is not unusual;[27b] however, the absence of exchange involving the σ,π-bound vinyl ligand was quite unexpected and appears to be an unusual feature of these diiron phosphido bridged alkenyl complexes. We have previously observed rapid fluxional behavior of the hydrocarbyl bridging ligand in the related acetylide $Fe_2(CO)_6(\mu\text{-}PPh_2)(\mu_2\text{-}\eta^1\text{:}\eta^2\text{-}C{\equiv}CR)$ which renders all carbonyl groups equivalent at room temperature, in sharp contrast to the observations reported here. Similar results to those of the acetylides have recently been described for the complex $Fe_2(CO)_6(\mu\text{-}SR)(\mu_2\text{-}\eta^1\text{:}\eta^2\text{-}MeC{=}CH_2)$.[20a] This molecule, related in many respects to those reported here, displays magnetic equivalence of all of its carbonyl ligands at room temperature, while at low temperatures the presence of two broad resonances was interpreted as indicating nonequivalence of the two iron sites arising from slow σ–π alkenyl exchange and rapid trigonal rotation at both metals.

The unusually high barrier to σ,π-alkenyl exchange in complex **5** is not unique to the parent vinyl ligand. Com-

(26) (a) Cherkas, A. A.; Randall, L. H.; MacLaughlin, S. A.; Mott, G. N.; Taylor, N. J.; Carty, A. J. *Organometallics* **1988**, *7*, 969. (b) Cherkas, A. A.; Doherty, S.; Cleroux, M.; Hogarth, G.; Randall, L. H.; Breckenridge, S. M.; Taylor, N. J.; Carty, A. J. *Organometallics* **1992**, *11*, 1701.

(27) (a) Nucciarone, D.; Taylor, N. J.; Carty, A. J. *Organometallics* **1986**, *5*, 1179. (b) Patin, H.; Mignani, G.; Benoit, A.; McGlinchey, M. J. *J. Chem. Soc., Dalton Trans.* **1981**, 1278.

(28) (a) Bruce, M. I.; Koutsantonis, G. A.; Tiekink, E. R. T. *J. Organomet. Chem.* **1991**, *407*, 391. (b) Corrigan, J. F.; Doherty, S.; Taylor, N. J.; Carty, A. J. *Organometallics*, in press.

(29) Randall, L. H.; Cherkas, A. A.; Carty, A. J. *Organometallics* **1989**, *8*, 568.

Table III. Crystal and Intensity Data for $Fe_2(CO)_6(\mu\text{-}PPh_2)(\mu_2\text{-}\eta^1\text{:}\eta^2\text{-}CH{=}CH_2)$ (5) and $Fe_2(CO)_6(\mu\text{-}PPh_2)(\mu_2\text{-}\eta^1\text{:}\eta^2\text{-}C(MeC{\equiv}C){=}CHMe)$ (10)

	5	10
formula	$C_{20}H_{13}Fe_2O_6P$	$C_{24}H_{17}O_6PFe_2$
mol wt	491.98	544.08
cryst class	monoclinic	monoclinic
space group	$P2_1/c$	$P2_1/n$
a (Å)	14.695 (4)	10.966 (2)
b (Å)	11.410 (2)	13.082 (3)
c (Å)	12.167 (3)	16.180 (2)
β (deg)	92.90 (1)	90.35 (1)
V (Å^3)	2037.5 (8)	2320.6 (8)
Z	4	4
d_{cal} (g cm^{-3})	1.604	1.56
F(000)	992	1104
radiation (Å)	0.71073	0.71073
temp (K)	295	180
μ(Mo Kα), cm^{-1}	15.33	13.54
diffractometer	Siemens R3m/v, 0.12 (100) × 0.13 (−100) × 0.27 (11−1) × 0.27 (−1−11) × 0.22 (−111) × 0.22 (1−1−1) distances from common center	Siemens R3m/v, 0.32 × 0.44 × 0.45
cryst size (mm)		
scan type	ω	2θ–θ
2θ range (deg)	3.5–50.0	3.5–55.0
scan width (deg)	1.20	0.9° below $K_{\alpha 1}$ to 0.9° above $K_{\alpha 2}$
scan speed (deg min^{-1})	2.93–29.30	3.66–29.30
abs corrections	face indexed numerical	ψ
transm factors	0.48–0.72	0.43–0.51
reflns measd	3934	5362
reflns obsd ($F \geq 6\sigma(F)$)	2902	4397
R	0.028	0.028
R_w	0.027	0.033
weighting scheme, w^{-1}	$\sigma^2(F)$	$\sigma^2(F) + 0.00001F^2$
max residuals, e A^{-3}	0.33, −0.27	0.27, −0.24

plexes **4a**, **3a**, **3b**, **7a**, and **8** show similar behavior. This contrasts with many reports of facile σ,π-alkenyl windshield wiper type motion on bi- and trinuclear metal complexes, there being only a single example of a similarly high-energy process in the recently reported complex $Fe_2(CO)_4(\mu\text{-}PPh_2)(\mu\text{-}dppm)(\mu_2\text{-}\eta^1\text{:}\eta^2\text{-}CH{=}CH_2)$. Since this contrasting behavior appears to be general for many diiron phosphido bridged alkenyl complexes (but not for the corresponding alkynyl complexes), we are currently performing a full kinetic study of the exchange process to try and understand the origin of these discrepancies.

X-ray Structures of $Fe_2(CO)_6(\mu\text{-}PPh_2)(\mu_2\text{-}\eta^1\text{:}\eta^2\text{-}CH{=}CH_2)$ (5) and $Fe_2(CO)_6(\mu\text{-}PPh_2)(\mu_2\text{-}\eta^1\text{:}\eta^2\text{-}C(C{\equiv}CMe){=}CHMe)$ (10)

The spectroscopic features of **5** have been utilised in determining the stereochemistry of hydrometalation of **1** with unsymmetrical alkynes. Although we confidently assigned the structure of the parent vinyl complex **5**, there remained the possibility of exo–endo isomerism with respect to the phosphido bridge (E, F). Thus we performed

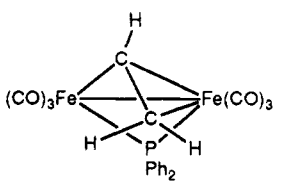

E, endo isomer

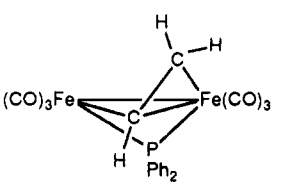

F, exo isomer

a single-crystal X-ray structure analysis of **5** to unambiguously assign the stereochemistry of the vinyl ligand with respect to the Fe_2P triangle. A perspective view of the molecular structure of **5** together with the atomic numbering scheme is illustrated in Figure 3. Bond distances and angles are given in Table VI. Although the spectroscopic features of **10** were consistent with the presence of a μ–σ,π-alkenyl ligand having a pendant unsaturated functionality attached to C_α, a single-crystal X-ray crystallographic analysis was carried out to provide precise details of the polyunsaturated fragment bound to the Fe_2 moiety. A perspective view of the molecular structure together with the atomic numbering scheme is illustrated in Figure 4. Bond distances and angles for this molecule are given in Table VII. Both of these structures are of high precision even by contemporary standards and the structure of **10** is one of the most precise X-ray structural

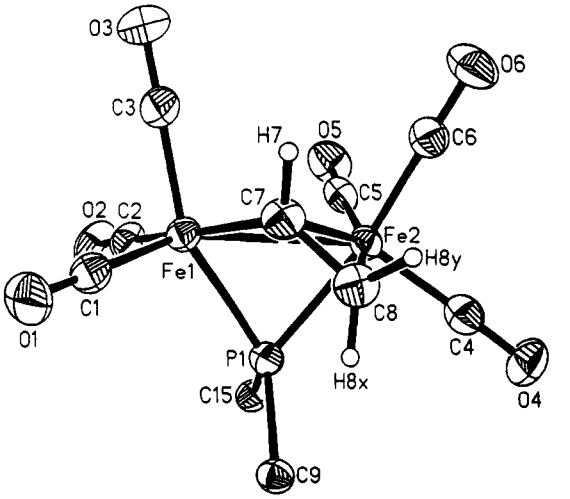

Figure 3. Perspective view of the molecular structure of the vinyl complex $Fe_2(CO)_6(\mu\text{-}PPh_2)(\mu_2\text{-}\eta^1\text{:}\eta^2\text{-}CH{=}CH_2)$ (**5**, phenyl rings omitted for clarity).

Table IV. Atomic Coordinates (×10^4) and Equivalent Isotropic Displacement Coefficients (Å × 10^3) for $Fe_2(CO)_6(\mu\text{-}PPh_2)(\mu_2\text{-}\eta^1\text{:}\eta^2\text{-}CH{=}CH_2)$ (5)

	x	y	z	U(eq)[a]
Fe(1)	2238.5 (3)	−883.1 (3)	3145.4 (3)	43.5 (1)
Fe(2)	1147.5 (3)	811.8 (3)	2534.2 (3)	42.5 (1)
P(1)	2560.7 (5)	500.3 (6)	1948.5 (5)	38.6 (2)
O(1)	3814 (2)	−1127 (2)	4672 (2)	81 (1)
O(2)	2559 (2)	−2631 (2)	1426 (2)	80 (1)
O(3)	1035 (2)	−2542 (2)	4223 (2)	85 (1)
O(4)	971 (2)	3104 (2)	1462 (2)	83 (1)
O(5)	273 (2)	−920 (2)	1046 (2)	76 (1)
O(6)	−570 (2)	924 (2)	3661 (2)	89 (1)
C(1)	3213 (2)	−1048 (3)	4040 (2)	56 (1)
C(2)	2430 (2)	−1961 (3)	2090 (2)	53 (1)
C(3)	1493 (2)	−1890 (3)	3821 (2)	56 (1)
C(4)	1026 (2)	2198 (3)	1861 (2)	55 (1)
C(5)	648 (2)	−246 (3)	1601 (2)	53 (1)
C(6)	98 (2)	868 (3)	3229 (3)	57 (1)
C(7)	1771 (2)	381 (3)	4057 (2)	52 (1)
C(8)	1876 (3)	1576 (3)	3955 (2)	56 (1)
C(9)	3456 (2)	1603 (2)	2160 (2)	42 (1)
C(10)	4089 (2)	1571 (3)	3042 (2)	57 (1)
C(11)	4769 (2)	2404 (3)	3166 (3)	70 (1)
C(12)	4816 (2)	3279 (3)	2406 (3)	68 (1)
C(13)	4202 (3)	3334 (3)	1519 (3)	67 (1)
C(14)	3525 (2)	2504 (3)	1397 (3)	56 (1)
C(15)	2727 (2)	132 (2)	512 (2)	42 (1)
C(16)	3561 (3)	−327 (3)	233 (3)	66 (1)
C(17)	3735 (3)	−583 (3)	−841 (3)	82 (2)
C(18)	3092 (4)	−371 (4)	−1642 (3)	85 (2)
C(19)	2269 (4)	83 (4)	−1405 (3)	82 (2)
C(20)	2076 (2)	327 (3)	−317 (3)	56 (1)

[a] Equivalent isotropic U defined as one-third of the trace of the orthogonalized U_{ij} tensor.

Table V. Atomic Coordinates (×10⁴) and Equivalent Isotropic Displacement Coefficients (Å × 10³) for $Fe_2(CO)_6(\mu\text{-}PPh_2)(\mu_2\text{-}\eta^1\text{:}\eta^2\text{-}C(C{\equiv}CMe){=}CHMe)$ (10)

	x	y	z	U(eq)[a]
Fe(1)	-253.8 (3)	4047.1 (2)	1773.0 (2)	22.36 (9)
Fe(2)	65.1 (3)	2215.3 (2)	2343.9 (2)	21.39 (9)
P(1)	1037.1 (5)	2908.8 (4)	1258.3 (3)	21.7 (2)
O(1)	1178 (2)	5927 (1)	1902 (1)	42.7 (6)
O(2)	-2617 (2)	4801 (2)	2404 (1)	47.8 (7)
O(3)	-1354 (2)	4262 (2)	116 (1)	46.7 (7)
O(4)	1438 (2)	313 (1)	2135 (1)	37.8 (6)
O(5)	-1116 (2)	1489 (2)	3862 (1)	45.3 (6)
O(6)	-2254 (2)	1894 (1)	1472 (1)	43.8 (6)
C(1)	618 (2)	5193 (2)	1832 (1)	29.6 (7)
C(2)	-1692 (2)	4499 (2)	2202 (1)	30.5 (7)
C(3)	-918 (2)	4163 (2)	758 (2)	30.0 (7)
C(4)	901 (2)	1055 (2)	2222 (1)	25.2 (6)
C(5)	-677 (2)	1805 (2)	3278 (2)	30.0 (7)
C(6)	-1327 (2)	2047 (2)	1783 (2)	29.0 (7)
C(7)	1791 (3)	2754 (2)	3930 (2)	36.0 (8)
C(8)	1419 (2)	3085 (2)	3069 (1)	26.7 (7)
C(9)	360 (2)	3652 (2)	2902 (1)	23.4 (6)
C(10)	-363 (2)	4000 (2)	3588 (1)	25.9 (6)
C(11)	-996 (2)	4344 (2)	4121 (1)	28.4 (7)
C(12)	-1805 (3)	4765 (3)	4746 (2)	39.5 (9)
C(13)	760 (2)	2394 (2)	219 (1)	24.2 (6)
C(14)	1269 (2)	2877 (2)	-462 (2)	33.5 (8)
C(15)	1054 (3)	2517 (2)	-1257 (2)	39.5 (8)
C(16)	328 (3)	1669 (2)	-1378 (2)	38.5 (8)
C(17)	-174 (2)	1175 (2)	-712 (2)	35.4 (8)
C(18)	39 (2)	1532 (2)	88 (2)	29.7 (7)
C(19)	2700 (2)	3073 (2)	1235 (1)	25.2 (7)
C(20)	3204 (2)	4021 (2)	1068 (2)	34.1 (8)
C(21)	4467 (3)	4116 (3)	978 (2)	44.2 (9)
C(22)	5214 (2)	3278 (3)	1062 (2)	44.2 (9)
C(23)	4715 (2)	2329 (2)	1231 (2)	44.3 (9)
C(24)	3463 (2)	2230 (2)	1319 (2)	35.0 (8)

[a] Equivalent isotropic U defined as one third of the trace of the orthogonalized U_{ij} tensor.

Table VI. Selected Interatomic Bond Distances (Å) and Angles (deg) for $Fe_2(CO)_6(\mu\text{-}PPh_2)(\mu_2\text{-}\eta^1\text{:}\eta^2\text{-}CH{=}CH_2)$ (5) with Esd's in Parentheses

Fe(1)-Fe(2)	2.597 (1)	Fe(1)-P(1)	2.215 (1)
Fe(1)-C(1)	1.764 (3)	Fe(1)-C(2)	1.810 (3)
Fe(1)-C(3)	1.813 (3)	Fe(1)-C(7)	1.964 (3)
Fe(2)-P(1)	2.258 (1)	Fe(2)-C(4)	1.786 (3)
Fe(2)-C(5)	1.789 (3)	Fe(2)-C(6)	1.798 (3)
Fe(2)-C(7)	2.084 (3)	Fe(2)-C(8)	2.169 (3)
P(1)-C(9)	1.830 (3)	P(1)-C(15)	1.826 (3)
O(1)-C(1)	1.145 (4)	O(2)-C(2)	1.135 (4)
O(3)-C(3)	1.130 (4)	O(4)-C(4)	1.143 (4)
O(5)-C(5)	1.145 (4)	O(6)-C(6)	1.138 (4)
C(7)-C(8)	1.379 (5)	C(9)-C(10)	1.384 (4)
C(9)-C(14)	1.392 (4)	C(10)-C(11)	1.382 (5)
C(11)-C(12)	1.365 (5)	C(12)-C(13)	1.372 (5)
C(13)-C(14)	1.377 (5)	C(15)-C(16)	1.390 (5)
C(15)-C(20)	1.373 (4)	C(16)-C(17)	1.375 (6)
C(17)-C(18)	1.353 (6)	C(18)-C(19)	1.363 (7)
C(19)-C(20)	1.396 (5)		
Fe(2)-Fe(1)-P(1)	55.3 (1)	Fe(2)-Fe(1)-C(1)	136.6 (1)
P(1)-Fe(1)-C(1)	106.7 (1)	Fe(2)-Fe(1)-C(2)	114.7 (1)
P(1)-Fe(1)-C(2)	88.4 (1)	C(1)-Fe(1)-C(2)	102.4 (1)
Fe(2)-Fe(1)-C(3)	102.9 (1)	P(1)-Fe(1)-C(3)	154.7 (1)
C(1)-Fe(1)-C(3)	98.2 (1)	C(2)-Fe(1)-C(3)	90.6 (1)
Fe(2)-Fe(1)-C(7)	52.2 (1)	P(1)-Fe(1)-C(7)	86.6 (1)
C(1)-Fe(1)-C(7)	91.5 (1)	C(2)-Fe(1)-C(7)	166.1 (1)
C(3)-Fe(1)-C(7)	88.4 (1)	Fe(1)-Fe(2)-P(1)	53.8 (1)
Fe(1)-Fe(2)-C(4)	146.8 (1)	P(1)-Fe(2)-C(4)	93.8 (1)
Fe(1)-Fe(2)-C(5)	84.6 (1)	P(1)-Fe(2)-C(5)	92.7 (1)
C(4)-Fe(2)-C(5)	106.2 (1)	Fe(1)-Fe(2)-C(6)	115.1 (1)
P(1)-Fe(2)-C(6)	168.3 (1)	C(4)-Fe(2)-C(6)	96.7 (1)
C(5)-Fe(2)-C(6)	89.3 (1)	Fe(1)-Fe(2)-C(7)	48.1 (1)
P(1)-Fe(2)-C(7)	82.7 (1)	C(4)-Fe(2)-C(7)	130.2 (1)
C(5)-Fe(2)-C(7)	123.6 (1)	C(6)-Fe(2)-C(7)	86.5 (1)
Fe(1)-Fe(2)-C(8)	78.4 (1)	P(1)-Fe(2)-C(8)	83.7 (1)
C(4)-Fe(2)-C(8)	92.5 (1)	C(5)-Fe(2)-C(8)	161.3 (1)
C(6)-Fe(2)-C(8)	90.6 (1)	C(7)-Fe(2)-C(8)	37.8 (1)
Fe(1)-P(1)-Fe(2)	71.0 (1)		

analyses of a $\mu\text{-}\eta^1\text{:}\eta^2$-alkenyl complex reported to date.

In molecule **5** the vinyl group is π-bound to Fe(2) [Fe(2)-C(7) = 2.084 (3) Å and Fe(2)-C(8) = 2.169 (3) Å] and σ-bound to Fe(1) [Fe(1)-C(7) = 1.964 (3) Å]. The C(7)-C(8) bond length [1.379 (5) Å] is comparable to the values of 1.396 (4) Å in $[Os_3(\mu\text{-}H)(\mu\text{-}\eta^1\text{:}\eta^2\text{-}CH{=}CH_2)(\mu\text{-}PPh_2)(CO)_7]$[30a] and 1.371 (7) Å in $[Mn_2(\mu_2\text{-}\eta^1\text{:}\eta^2\text{-}CH{=}CH_2)(\mu\text{-}PPh_2)(CO)_7]$,[30b] showing the expected increase in C-C bond length upon coordination to a metal center. The two $Fe(CO)_3$ units adopt a staggered arrangement with respect to each other, which may be attributed to the steric interaction of the exo-vinylic CH_2 unit with the carbonyl ligands. Both metal centers obey the 18-electron rule provided that the electronic imbalance associated with the presence of the hydrocarbyl bridge is counteracted by a two-electron-donor interaction of the phosphido bridge to Fe(1). This asymmetry in the electron-donor properties of the phosphido bridge is reflected in the nonequivalence of Fe(1)-P(1) and Fe(2)-P(1) [Fe(1)-P(1) 2.215 (1) Å and Fe(2)-P(1) = 2.258 (1) Å]; the stronger interaction is to the electron-poor metal atom. Ignoring the metal-metal bond, Fe(2) may be considered as five coordinate with pseudo-trigonal-bipyramidal geometry, the η^2 interaction of the vinyl ligand occupying a single coordination site. The atom Fe(1) can be seen to have a similar trigonal-bipyramidal geometry, the only difference being in the ligands contained in the equatorial and axial positions. At Fe(1) the trigonal plane is defined by the two carbonyl ligands CO(1) and CO(3) and the phosphido bridge phosphorus atom, while the apical sites contain CO(2) and C(7) [angle C(2)-Fe(1)-C(7) = 166.1 (1)°]. Conversely, the equivalent trigonal plane of Fe(2) constitutes CO(5), CO(4), and the midpoint of the η^2 interaction of the vinyl ligand, while P(1) and CO(6) occupy the apical positions [angle P(1)-Fe(1)-C(6) = 168.3 (1)°].

The X-ray structure of **10** confirms that cis hydrodimetalation of a single alkyne unit has occurred, affording a pendant propynyl group bound to C_α of the $\mu\text{-}\eta^1\text{:}\eta^2$-alkenyl ligand.

The molecule contains a short Fe-Fe single bond (Fe(1)-Fe(2) = 2.591 (1) Å) consistent with other values reported for diiron units bridged by vinyl ligands, and a slightly asymmetrical phosphido bridge (Fe(1)-P(1) = 2.221 (1) Å, Fe(2)-P(1) = 2.251 (1) Å). The nature of the polyunsaturated hydrocarbyl ligand is of interest. The C(8)-C(9) (alkenyl) bond length (1.410 (3) Å) and the metal-alkenyl distances Fe(1)-C(9) = 2.011 (2) Å, Fe(2)-C(9) = 2.109 (2) Å, Fe(2)-C(8) = 2.204 (2) Å) are characteristic of metal-alkenyl bonding modes. Recently we found[28b] that uncoordinated alkyne fragments exhibited C≡C bond lengths in the range 1.176 (10)-1.189 (5) Å. The C-C bond length of the free acetylenic fragment in **10** [C(10)-C(11) 1.201 (3) Å] is in agreement with these and with other literature[28a] values being typical of a free carbon-carbon triple bond [HC≡CH = 1.20 Å]. The C-C bond linking the two unsaturated fragments is short [C(9)-C(10) = 1.438 (2) Å], presumably reflecting the high "s" character of the sp-sp^2 bond and delocalization over the enyne fragment as suggested by the ^{13}C NMR data. The conformation of the coordinated alkenyl group, with a C(7)-C(8)-C(9)/C(8)-C(9)-C(10) dihedral angle of 4.7° is in keeping with a metal-(metallaolefin) or metal-(metalla-allyl) description of the Fe_2C_2 framework. As

(30) Herberich, G. E.; Mayer, H. J. J. Organomet. Chem. 1988, 347, 93.

Table VII. Selected Interatomic Bond Distances (Å) and Angles (deg) for $Fe_2(CO)_6(\mu\text{-}PPh_2)(\mu_2\text{-}\eta^1\text{:}\eta^2\text{-}C(C{\equiv}CMe){=}CHMe)$ (10) with Esd's in Parentheses

Fe(1)–Fe(2)	2.591 (1)	Fe(1)–P(1)	2.220 (1)
Fe(1)–C(1)	1.780 (2)	Fe(1)–C(2)	1.825 (2)
Fe(1)–C(3)	1.798 (2)	Fe(1)–C(9)	2.010 (2)
Fe(2)–P(1)	2.251 (1)	Fe(2)–C(4)	1.785 (2)
Fe(2)–C(5)	1.803 (2)	Fe(2)–C(6)	1.785 (2)
Fe(2)–C(8)	2.203 (2)	Fe(2)–C(9)	2.109 (2)
P(1)–C(13)	1.835 (2)	P(1)–C(19)	1.836 (2)
O(1)–C(1)	1.146 (3)	O(2)–C(2)	1.138 (3)
O(3)–C(3)	1.149 (3)	O(4)–C(4)	1.145 (3)
O(5)–C(5)	1.140 (3)	O(6)–C(6)	1.149 (3)
C(7)–C(8)	1.511 (3)	C(8)–C(9)	1.404 (3)
C(9)–C(10)	1.442 (3)	C(10)–C(11)	1.198 (3)
C(11)–C(12)	1.458 (4)	C(13)–C(14)	1.391 (3)
C(13)–C(18)	1.392 (3)	C(14)–C(15)	1.388 (4)
C(15)–C(16)	1.379 (4)	C(16)–C(17)	1.374 (4)
C(17)–C(18)	1.395 (4)	C(19)–C(20)	1.385 (3)
C(19)–C(24)	1.391 (3)	C(20)–C(21)	1.399 (4)
C(21)–C(22)	1.375 (4)	C(22)–C(23)	1.384 (4)
C(23)–C(24)	1.388 (4)		
Fe(2)–Fe(1)–P(1)	55.1 (1)	Fe(2)–Fe(1)–C(1)	133.5 (1)
P(1)–Fe(1)–C(1)	104.0 (1)	Fe(2)–Fe(1)–C(2)	106.2 (1)
P(1)–Fe(1)–C(2)	156.1 (1)	C(1)–Fe(1)–C(2)	99.9 (1)
Fe(2)–Fe(1)–C(3)	117.1 (1)	P(1)–Fe(1)–C(3)	88.2 (1)
C(1)–Fe(1)–C(3)	101.1 (1)	C(2)–Fe(1)–C(3)	88.5 (1)
Fe(2)–Fe(1)–C(9)	52.7 (1)	P(1)–Fe(1)–C(9)	87.6 (1)
C(1)–Fe(1)–C(9)	89.5 (1)	C(2)–Fe(1)–C(9)	91.3 (1)
C(3)–Fe(1)–C(9)	169.3 (1)	Fe(1)–Fe(2)–P(1)	54.0 (1)
Fe(1)–Fe(2)–C(4)	144.6 (1)	P(1)–Fe(2)–C(4)	90.6 (1)
Fe(1)–Fe(2)–C(5)	120.9 (1)	P(1)–Fe(2)–C(5)	173.0 (1)
C(4)–Fe(2)–C(5)	94.3 (1)	Fe(1)–Fe(2)–C(6)	79.6 (1)
P(1)–Fe(2)–C(6)	93.5 (1)	C(4)–Fe(2)–C(6)	106.1 (1)
C(5)–Fe(2)–C(6)	90.0 (1)	Fe(1)–Fe(2)–C(8)	78.6 (1)
P(1)–Fe(2)–C(8)	83.5 (1)	C(4)–Fe(2)–C(8)	98.8 (1)
C(5)–Fe(2)–C(8)	90.7 (1)	C(6)–Fe(2)–C(8)	155.0 (1)
Fe(1)–Fe(2)–C(9)	49.3 (1)	P(1)–Fe(2)–C(9)	84.4 (1)
C(4)–Fe(2)–C(9)	136.7 (1)	C(5)–Fe(2)–C(9)	88.6 (1)
C(6)–Fe(2)–C(9)	117.1 (1)	C(8)–Fe(2)–C(9)	37.9 (1)
Fe(1)–P(1)–Fe(2)	70.8 (1)	Fe(1)–P(1)–C(13)	119.2 (1)
Fe(2)–P(1)–C(13)	119.4 (1)	Fe(1)–P(1)–C(19)	124.4 (1)
Fe(2)–P(1)–C(19)	122.6 (1)	C(13)–P(1)–C(19)	100.5 (1)
Fe(1)–C(1)–O(1)	177.4 (2)	Fe(1)–C(2)–O(2)	174.3 (2)
Fe(1)–C(3)–O(3)	178.1 (2)	Fe(2)–C(4)–O(4)	179.3 (2)
Fe(2)–C(5)–O(5)	175.9 (2)	Fe(2)–C(6)–O(6)	174.7 (2)
Fe(2)–C(8)–C(7)	121.3 (2)	Fe(2)–C(8)–C(9)	67.4 (1)
C(7)–C(8)–C(9)	123.2 (2)	Fe(1)–C(9)–Fe(2)	77.9 (1)
Fe(1)–C(9)–C(8)	125.7 (2)	Fe(2)–C(9)–C(8)	74.7 (1)
Fe(1)–C(9)–C(10)	115.9 (2)	Fe(2)–C(9)–C(10)	121.8 (2)
C(8)–C(9)–C(10)	118.4 (2)	C(9)–C(10)–C(11)	175.1 (2)
C(10)–C(11)–C(12)	177.8 (3)		

illustrated in Figure 4, the alkynyl group is relatively unhindered and should be quite accessible for further chemical transformation.

Conclusion

In summary, we have shown that diiron alkenyl complexes are readily accessible via the cis hydrodimetalation of a single alkyne unit. This reaction occurs with a high regiospecificity affording the isomer in which the bulky substituent is located on C_α of the $\mu\text{-}\sigma,\pi$-vinyl ligand. In the case of diynes this synthetic procedure has afforded the first $\mu\text{-}\sigma,\pi$-alkenyl ligands with pendant alkynyl functionality attached to C_α. Although the generation of new polymers with polymetallic fragments in the backbone, or as functional groups, is in its infancy, the ready availability of compounds such as **2**–**11** illustrates the potential of this method. The steric environment of the polymerisable moieties and the generation of organometallics radicals which may cause termination of polymer chain reactions are potential difficulties. In this regard the unhindered environment of the pendant alkynyl group in **10** and the ability of related diiron complexes to serve as radical initiators suggests that molecules such as **10** and **11b** should be ideally suitable for polymer incorporation.

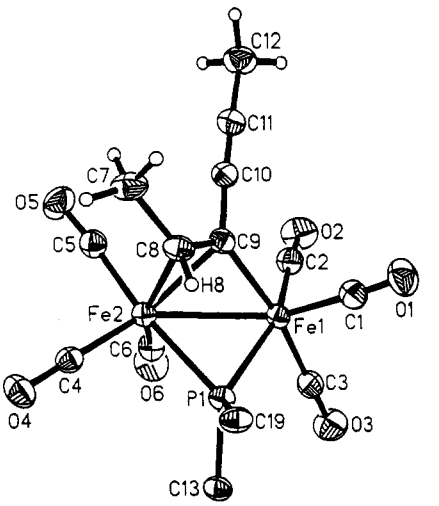

Figure 4. Perspective view of the molecular structure of $Fe_2(CO)_6(\mu\text{-}PPh_2)(\mu_2\text{-}\eta^1\text{:}\eta^2\text{-}C(C{\equiv}CMe){=}CHMe)$ (**10**, phenyl rings omitted for clarity).

Experimental Section

General Procedures. Standard Schlenk line techniques were employed, and all reactions were carried out under an atmosphere of dry nitrogen. Hexane and diethyl ether were distilled under nitrogen from sodium/benzophenone ketyl prior to use. Acetylenes were purchased from Farchan Laboratories and purified by distillation under nitrogen before being used.

All reactions were monitored by thin-layer chromatography (Baker Flex, silica Gel 1B-F). Purification of products was accomplished by column chromatography using silica gel (70–230 mesh) with the total exclusion of air and moisture. Solution infrared spectra (NaCl solution cells) were recorded on a Nicolet 520 FTIR spectrometer. Proton NMR spectra were recorded on Bruker AC-200, AM-250 instruments, and chemical shifts are referenced internally to Me_4Si. $^{13}C\{^1H\}$ NMR spectra were recorded on Bruker AC-200 or AM-250 spectrometers operating at 50.32 and 62.97 MHz, respectively, and referenced internally to Me_4Si. Broad-band proton decoupled ^{31}P NMR spectra were also obtained with a Bruker AC-200 or AM-250 operating at 81.02 and 101.27 MHz, respectively, and using a solution of 85% aqueous H_3PO_4 as an external reference. Microanalyses were performed by M-H-W Laboratories, Phoenix, AZ.

Synthesis and Characterization. *Preparation of $HFe_2(CO)_7(\mu\text{-}PPh_2)$ (1).* A solution of $Fe_2(CO)_8(\mu\text{-}PPh_2)]^-Na^+$ (1.5 THF) (3.69 g, 5.65 mmol) in dichloromethane (15 mL) was treated dropwise with tetrafluoroboric acid (85%, 0.982 mL, 5.9 mmol) at −78 °C. After addition of acid was complete, the solution was stirred vigorously for 30 min and then left to warm to room temperature slowly. During this time CO evolution was apparent and the reaction mixture finally turned black-red. This method was used for the in situ preparation of **1** which was reacted with alkynes, no further purification being necessary. IR (ν(CO) cm^{-1}, C_6H_{14}): 2091 m, 2040 s, 2027 vs, 2020 s,sh, 2001 s, 1977 m. ^1H NMR (200 MHz, C_6D_6, δ): 6.9–7.7 (m, C_6H_5, 10 H), −9.98 (d, $^2J_{PH}$ = 53.9 Hz, Fe–*H*, 1 H). $^{31}P\{^1H\}$ NMR (81.02 MHz, $(CD_3)_2CO$, 298 K, δ): 170.43 (s). $^{13}C\{^1H\}$ NMR (50.32 MHz, C_6D_6, 298 K, δ): 211.1 (s, br, CO), 139.2 (d, br, $^1J_{PC}$ = 30.2 Hz, ipso), 123.9 (s, br, ortho), 130.4 (s, para), 128.7 (d, $^3J_{PC}$ = 10.1 Hz, meta).

Preparation of $Fe_2(CO)_6(\mu\text{-}PPh_2)(\mu_2\text{-}\eta^1\text{:}\eta^2\text{-}C(C{\equiv}CMe){=}CHMe)$ (10). A solution of $HFe_2(CO)_7(\mu\text{-}PPh_2)$ (0.317 g, 0.642 mmol) in diethyl ether (20 mL) was treated with 2,4-hexadiyne (0.050 g, 0.642 mmol) in diethyl ether (1 mL). A brisk evolution of gas was observed slowing gradually over the course of the reaction. IR monitoring of the ν(CO) bands showed the reaction to be complete after approximately 7 h. The mixture was absorbed onto silica gel, dried under reduced pressure, and then subjected to purification by column chromatography. Elution with hexane

yielded one major band. The eluant was filtered and concentrated in vacuo to ~5 mL and stored at −10 °C yielding orange crystals of $Fe_2(CO)_6(\mu\text{-}PPh_2)(\mu\text{-}\eta^1{:}\eta^2\text{-}C(C{\equiv}CMe){=}CHMe)$ (**10**, 0.202 g, 55%). Anal. Calcd for $C_{24}H_{17}O_6PFe_2$: C, 52.98; H, 3.15; P, 5.69. Found: C, 52.99; H, 3.17; P, 5.76. IR (ν(CO), cm^{-1}, C_6H_{12}): 2063 m, 2030 vs, 1998 m, 1990 w, 1981 s, 1967 vw. ^1H NMR (200 MHz, $CDCl_3$, δ): 6.9–7.7 (m, C_6H_5, 10 H), 2.87 (dq, $^2J_{CH}$ = 5.8 Hz, $^3J_{PH}$ = 6.1 Hz, C=C*H*Me, 1 H), 2.01 (s, C≡CCH_3, 3 H), 1.48 (d, $^3J_{CH}$ = 5.8 Hz, C=CHCH_3, 3 H). $^{31}P\{^1H\}$ NMR (81.02 MHz, $CDCl_3$, δ): 166.43 (s). ^{13}C NMR (50.32 MHz, $CDCl_3$, δ): 211 (m, br, CO), 153.02 (d, $^2J_{PC}$ = 24.5 Hz, *C*=CHCH$_3$), 100.90 (q, $^2J_{CH}$ = 10.7 Hz, C≡*C*CH$_3$), 90.87 (d, $^3J_{PC}$ = 4.8 Hz, *C*≡CCH$_3$), 86.82 (dd, $^2J_{PC}$ = 15.3 Hz, $^1J_{CH}$ = 164.9 Hz, C=*C*HCH$_3$), 22.57 (dq, $^3J_{CP}$ = 5.9 Hz, $^1J_{CH}$ = 122.5 Hz, C≡CH*C*H$_3$), 4.87 (q, $^1J_{CH}$ = 131.4 Hz, C≡*C*CH$_3$).

The following other μ-σ,π-alkenyl complexes were prepared by a similar procedure. Selected spectroscopic data are listed for each of the compounds **2–9** and **11**.

$Fe_2(CO)_6(\mu\text{-}PPh_2)(\mu_2\text{-}\eta^1{:}\eta^2\text{-}C(TMS){=}CH_2)$ (***2a***). Obtained as orange crystals in 66% yield from dichloromethane/*n*-hexane at −10 °C. Anal. Calcd for $C_{23}H_{21}Fe_2O_6PSi$: C, 48.97; H, 3.75. Found: C, 49.11; H, 3.54. IR (ν(CO), cm^{-1}, C_6H_{12}): 2056 w, 2022 s, 1986 w, 1980 vw. ^1H NMR (200 MHz, $CDCl_3$, δ): 7.0–7.7 (m, C_6H_5, 10 H), 3.39 (dd, $^3J_{PH}$ = 12.6 Hz, $^2J_{HHgem}$ = 3.7 Hz, TMSC = $CH_{cis}H_{trans}$, 1 H), 2.70 (dd, $^3J_{PH}$ = 9.4 Hz, $^2J_{HHgem}$ = 3.7 Hz, TMSC = $H_{cis}H_{trans}$, 1 H), −0.22 (s, Si(CH_3)$_3$, 9 H). $^{31}P\{^1H\}$ NMR (81.02 MHz, $CDCl_3$, δ): 172.4 (s). $^{13}C\{^1H\}$ NMR (50.32 MHz, $CDCl_3$, δ): 212 (s, br, CO), 187.87 (d, $^2J_{PC}$ = 25.2 Hz, TMS*C*=CH$_2$), 75.25 (d, $^3J_{PC}$ = 17.1 Hz, TMSC=*C*H$_2$), −0.69 (s, Si(*C*H$_3$)$_3$).

$Fe_2(CO)_6(\mu\text{-}PPh_2)(\mu_2\text{-}\eta^1{:}\eta^2\text{-}CH{=}CH(TMS))$ (***2b***). Obtained as orange crystals in 6% yield from *n*-hexane at −10 °C. IR (ν(CO), cm^{-1}, C_6H_{12}): 2063 m, 2026 s, 1997 m, 1986 w, 1981 m. ^1H NMR (200 MHz, $CDCl_3$, δ): 8.62 (dd, $^3J_{HH}$ = 14.9 Hz, $^3J_{PH}$ = 3.7 Hz, *H*C=C(H)TMS, 1 H), 7.0–7.7 (m, C_6H_5, 10 H), 2.64 (dd, $^3J_{HH}$ = 14.9 Hz, $^3J_{PH}$ = 12.7 Hz, HC=(*H*)TMS, 1 H), −0.19 (s, Si(CH_3)$_3$, 9 H). $^{31}P\{^1H\}$ NMR (81.02 MHz, $CDCl_3$, δ): 171.9 (s). $^{13}C\{^1H\}$ NMR (50.32 MHz, $CDCl_3$, δ): 211 (s, br, CO), 164.23 (d, $^2J_{PC}$ = 26.4 Hz, H*C*=C(H)TMS), 88.61 (d, $^2J_{PC}$ = 12.3 Hz, HC=*C*(H)TMS), −0.84 (s, Si(*C*H$_3$)$_3$).

$Fe_2(CO)_6(\mu\text{-}PPh_2)(\mu_2\text{-}\eta^1{:}\eta^2\text{-}CPh{=}CH_2)$ (***3a***). Orange crystals in 56% yield from *n*-hexane at −10 °C. Anal. Calcd for $C_{26}H_{17}Fe_2O_6P$: C, 54.97; H, 3.02; P, 5.45. Found: C, 54.90; H, 3.06; P, 5.77. IR (ν(CO), cm^{-1}, C_6H_{12}): 2060 m, 2028 s, 1994 s, 1980 s, 1964 vw. ^1H NMR (200 MHz, $CDCl_3$, δ): 7.0–7.7 (m, C_6H_5, 15 H), 2.99 (dd, $^3J_{PH}$ = 14.7 Hz, $^2J_{HHgem}$ = 2.0 Hz, PhC=$CH_{cis}H_{trans}$, 1 H), 2.21 (dd, $^3J_{PH}$ = 10.3 Hz, $^2J_{HHgem}$ = 3.0 Hz, PhC=C$H_{cis}H_{trans}$, 1 H). $^{31}P\{^1H\}$ NMR (81.02 MHz, $CDCl_3$, δ): 168.33 (s). $^{13}C\{^1H\}$ NMR (50.32 MHz, $CDCl_3$, δ): 213.2 (s, br, CO), 208.9 (s, br CO), 189.04 (d, $^2J_{PC}$ = 20.1 Hz, PhC=CH$_2$), 66.19 (d, $^3J_{PC}$ = 13.3 Hz, CPh=*C*H$_2$).

$Fe_2(CO)_6(\mu\text{-}PPh_2)(\mu_2\text{-}\eta^1{:}\eta^2\text{-}CH{=}CHPh)$ (***3b***). Obtained as orange/red crystals in 16% yield from *n*-hexane at −10 °C. Anal. Calcd for $C_{26}H_{17}Fe_2O_6P$: C, 54.97; H, 3.02; P, 5.45. Found: C, 54.90; H, 3.12; P, 5.23. IR (ν(CO), cm^{-1}, C_6H_{12}): 2064 m, 2029 m, 1998 m, 1990 w, 1984 m, 1971 vw. ^1H NMR (200 MHz, $CDCl_3$, δ): 8.93 (dd, $^3J_{HHvic}$ = 13.4 Hz, $^3J_{PH}$ = 5.5 Hz, *H*C=CHPh, 1 H), 7.0–7.7 (m, C_6H_5, 15 H), 4.29 (dd, $^3J_{HHvic}$ = 13.4 Hz, $^3J_{PH}$ = 5.0 Hz, HC=C*H*Ph, 1 H), $^{13}C\{^1H\}$ NMR (50.32 MHz, $CDCl_3$, δ): 210 (s, br, CO), 145.74 (d, $^2J_{PC}$ = 27.1 Hz, *C*H=CHPh), 93.57 (d, $^3J_{PC}$ = 17.5 Hz, CH=*C*PhH).

$Fe_2(CO)_6(\mu\text{-}PPh_2)(\mu_2\text{-}\eta^1{:}\eta^2\text{-}C(C_6H_4C{\equiv}CH){=}CH_2)$ (***4a***). Obtained in 36% yield from *n*-hexane at −10 °C. Anal. Calcd for $C_{28}H_{17}Fe_2O_6P$: C, 56.80, H, 2.89; P, 5.27. Found: C, 56.79; H, 2.96; P, 5.41. IR (ν(CO), cm^{-1}, C_6H_{12}): 2061 w, 2029 vs, 1995 m, 1982 s, 1966 vw. ^1H NMR (200 MHz, $CDCl_3$, δ): 7.0–7.7 (m, C_6H_5, 14 H), 2.98 (dd, $^2J_{HHgem}$ = 3.1 Hz, $^3J_{PH}$ = 14.7 Hz, C=$CH_{cis}H_{trans}$, 1 H), 2.97 (s, C≡C*H*, 1 H), 2.22 (dd, $^2J_{HHgem}$ = 3.1 Hz, $^3J_{PH}$ = 10.2 Hz, C=C$H_{cis}H_{trans}$, 1 H). $^{31}P\{^1H\}$ NMR (81.02 MHz, $CDCl_3$, δ): 168.70 (s). ^{13}C NMR (50.32 MHz, $CDCl_3$, δ): 213.0 (d, br, $^2J_{PC}$ = 2.7 Hz, CO), 208.8 (s, br, CO), 186.93 (d, $^2J_{PC}$ = 19.9 Hz, *C*=CH$_2$), 83.55 (d, $^2J_{CH}$ = 49.2 Hz, *C*≡CH), 66.18 (ddd, $^3J_{PC}$ = 13.4 Hz, $^1J_{CH}$ = 153.1 Hz, 161.8 Hz, C=*C*H$_2$), 77.25 (s, $^1J_{CH}$ = 251.0 Hz, C≡*C*H).

$Fe_2(CO)_6(\mu\text{-}PPh_2)[\mu_2\text{-}\eta^1{:}\eta^2\text{-}CH{=}CH(C_6H_4C{\equiv}CH)]$ (***4b***). Obtained as red/orange crystals in 8% yield from *n*-hexane at −10 °C. ^1H NMR (200 MHz, $CDCl_3$, δ): 8.76 (dd, $^3J_{HHvic}$ = 13.5 Hz, $^3J_{PH}$ = 6.3 Hz, *H*C=CHPh, 1 H), 6.8–7.6 (m, C_6H_5 and C_6H_4-C≡CH, 14 H), 3.88 (dd, $^3J_{HHvic}$ = 13.6 Hz, $^3J_{PH}$ = 5.1 Hz, HC=C*H*Ph, 1 H), 2.97 (s, C≡C*H*, 1 H). $^{31}P\{^1H\}$ NMR (81.02 MHz, $CDCl_3$, δ): 169.07 (s).

$Fe_2(CO)_6(\mu\text{-}PPh_2)(\mu_2\text{-}\eta^1{:}\eta^2\text{-}CH{=}CH_2)$ (***5***). Orange crystals in 34% yield from *n*-hexane. Anal. Calcd for $C_{20}H_{13}Fe_2O_6P$: C, 48.83; H, 2.66; P, 6.29. Found: C, 48.75; H, 2.69; P, 6.85. IR (ν(CO), cm^{-1}, C_6H_{12}): 2065 m, 2029 vs, 1999 s, 1983 s, 1951 w, 1946 w. ^1H NMR (200 MHz, $CDCl_3$, δ): 8.32 (ddd, $^3J_{HHvic}$ = 13.4 Hz, $^3J_{PH}$ = 5.9 Hz, $^3J_{HHcis}$ = 9.6 Hz, *H*C=CH$_2$, 1 H), 7.0–7.7 (m, C_6H_5, 10 H), 3.32 (ddd, $^3J_{PH}$ = 11.7 Hz, $^3J_{HHcis}$ = 9.6 Hz, $^2J_{HHgem}$ = 2.1 Hz, HC=C$H_{cis}H_{trans}$, 1 H), 2.43 (ddd, $^3J_{HHvic}$ = 13.4 Hz, $^3J_{PH}$ = 6.7 Hz, $^2J_{HHgem}$ = 2.1 Hz, HC=C$H_{cis}H_{trans}$, 1 H). $^{31}P\{^1H\}$ NMR (81.02 MHz, $CDCl_3$, δ): 176.11 (s). $^{13}C\{^1H\}$ NMR (50.32 MHz, $CDCl_3$, δ): 212 (s, br, CO), 210 (s, br, CO), 158.78 (d, $^2J_{PC}$ = 26.9 Hz, HC=CH$_2$), 72.47 (d, $^3J_{PC}$ = 15.3 Hz, HC=*C*H$_2$).

$Fe_2(CO)_6(\mu\text{-}PPh_2)(\mu_2\text{-}\eta^1{:}\eta^2\text{-}CPh{=}CHPh)$ (***6***). Orange crystals in 52% yield from *n*-hexane. Anal. Calcd for $C_{32}H_{21}Fe_2O_6P$: C, 59.67; H, 3.29; P, 4.81. Found: C, 59.24; H, 3.11; P, 4.27. IR (ν(CO), cm^{-1}, C_6H_{12}): 2058 m, 2017 s, 1989 m, 1977 m, 1960 w. ^1H NMR (200 MHz, $CDCl_3$, δ): 7.0–7.7 (m, C_6H_5, 20 H), 3.75 (d, $^3J_{PH}$ = 8.7 Hz, PhC=C*H*Ph, 1 H). $^{31}P\{^1H\}$ NMR (81.02 MHz, $CDCl_3$, δ): 171.45 (s). $^{13}C\{^1H\}$ NMR (50.32 MHz, $CDCl_3$, δ): 213.0 (br, CO), 209 (v br, CO), 181.27 (d, $^2J_{PC}$ = 19.5 Hz, PhC=CHPh), 85.36 (d, $^3J_{PC}$ = 17.5 Hz, CPh=*C*HPh).

$Fe_2(CO)_6(\mu\text{-}PPh_2)(\mu_2\text{-}\eta^1{:}\eta^2\text{-}C(CH_2Cl){=}CH_2)$ (***7***). Obtained as yellow/orange crystals in 35% yield from *n*-hexane at −10 °C. Anal. Calcd for $C_{21}H_{14}ClFe_2O_6P$: C, 47.05; H, 2.63; P, 5.78. Found: C, 46.72; H, 2.70; P, 5.37. IR (ν(CO), cm^{-1}, C_6H_{12}): 2064 m, 2030 vs, 1995 sh, 1992 s, 1983 w, 1972 vw. ^1H NMR (200 MHz, $CDCl_3$, δ): 7.0–7.7 (m, C_6H_5, 10 H), 4.96 (AB, $^2J_{HaHb}$ = 11.5 Hz C-(CH_aH$_b$Cl), 1 H), 4.36 (AB, $^2J_{HaHb}$ = 11.5 Hz, C(CH$_a$H$_b$Cl), 1 H), 3.26 (dd, $^3J_{PH}$ = 15.1 Hz, $^2J_{HHgem}$ = 3.4 Hz, C(CH$_2$Cl)=C$H_{cis}H_{trans}$, 1 H), 2.19 (dd, $^3J_{PH}$ = 10.13 Hz, $^2J_{HHgem}$ = 3.4 Hz, C(CH$_2$Cl)=C$H_{cis}H_{trans}$, 1 H). $^{31}P\{^1H\}$ NMR (81.02 MHz, $CDCl_3$, δ): 172.28 (s). $^{13}C\{^1H\}$ NMR (50.32 MHz, $CDCl_3$, δ): 211.6 (s, br, CO), 208 (s, v br, CO), 178.06 (d, $^2J_{PC}$ = 21.4 Hz, *C*(CH$_2$Cl)=CH$_2$), 70.56 (d, $^3J_{PC}$ = 13.6 Hz, C(CH$_2$Cl)=*C*H$_2$), 63.85 (d, $^3J_{PC}$ = 4.50 Hz, C(*C*H$_2$Cl)=CH$_2$).

$Fe_2(CO)_6(\mu\text{-}PPh_2)(\mu_2\text{-}\eta^1{:}\eta^2\text{-}C(OEt){=}CH_2)$ (***8***). Isolated as orange crystals in 33% yield from *n*-hexane at −10 °C. Anal. Calcd for $C_{22}H_{17}Fe_2O_7P$: C, 49.30; H, 3.20. Found: C, 48.87; H, 3.23. IR (ν(CO), cm^{-1}, C_6H_{12}): 2066 m, 2029 s, 2000 m, 1986 m, 1980 s, 1967 vw. ^1H NMR (200 MHz, $CDCl_3$, δ): 7.0–7.7 (m, C_6H_5, 10 H), 3.76 (dq, $^2J_{HH}$ = 9.0 Hz, $^3J_{HH}$ = 6.9 Hz, CH_aH$_b$CH$_3$, 1 H), 3.67 (dq, $^2J_{HH}$ = 9.0 Hz, $^3J_{HH}$ = 6.9 Hz, CH$_a$H$_b$CH$_3$, 1 H), 2.77 (dd, $^3J_{PH}$ = 16.9 Hz, $^2J_{HHgem}$ = 5.70 Hz, C(OEt)=C$H_{cis}H_{trans}$, 1 H), 1.46 (dd, $^3J_{PH}$ = 11.8 Hz, $^2J_{HHgem}$ = 5.7 Hz, C(OEt)=C$H_{cis}H_{trans}$, 1 H), 1.23 (dd, $^2J_{HaH}$ = $^2J_{HbH}$ = 6.9 Hz, CH$_a$H$_b$CH_3, 3 H). $^{31}P\{^1H\}$ NMR (81.02 MHz, $CDCl_3$, δ): 161.64 (s). ^{13}C NMR (50.32 MHz, $CDCl_3$, δ): 220.30 (d, $^2J_{PC}$ = 20.2 Hz, *C*(OEt)=CH$_2$), 211.0 (s, br, CO), 209.1 (s, v br, CO), 67.18 (dd, $^1J_{CH}$ = 145.0 Hz, C(O*C*H$_2$CH$_3$)=CH$_2$), 47.96 (d, $^3J_{PC}$ = 8.9 Hz, C(OEt)=*C*H$_2$), 14.50 (q, $^1J_{CH}$ = 127.2 Hz, C(OCH$_2$*C*H$_3$)=CH$_2$).

$Fe_2(CO)_6(\mu\text{-}PPh_2)(\mu_2\text{-}\eta^1{:}\eta^2\text{-}C(CH_2CMe){=}CH_2)$ (***9***). Isolated as red/orange crystals in 42% yield from *n*-hexane at −10 °C. Anal. Calcd for $C_{22}H_{17}Fe_2O_6P$: C, 52.43; H, 3.40; P, 6.14. Found: C, 52.49; H, 3.48; P, 6.01. IR (ν(CO), cm^{-1}, C_6H_{12}): 2056 w, 2019 s, 1986 m, 1975 m, 1959 w. ^1H NMR (200 MHz, $CDCl_3$, δ): 7.0–7.7 (m, C_6H_5, 10 H), 4.84 (AB, $^2J_{AB}$ < 1.5 Hz, C(CH_aH$_b$CMe)=CH$_2$, 1 H), 4.77 (AB, $^2J_{AB}$ < 1.5 Hz, C(CH$_a$H$_b$CMe)=CH$_2$, 1 H), 2.70 (dd, $^2J_{HHgem}$ = 3.7 Hz, $^3J_{PH}$ = 14.7 Hz, C=CH$_{cis}H_{trans}$, 1 H), 2.02 (dd, $^3J_{HHgem}$ = 3.7 Hz, $^3J_{PH}$ = 9.8 Hz, C=C$H_{cis}H_{trans}$, 1 H), 1.83 (s, C(CH$_2$CCH_3)=CH$_2$, 3 H). $^{31}P\{^1H\}$ NMR (81.02 MHz, $CDCl_3$, δ): 173.13 (s). $^{13}C\{^1H\}$ NMR (50.32 MHz, $CDCl_3$, δ): 210 (m, br, CO), 194.33 (d, $^2J_{PC}$ = 20.6 Hz, *C*=CH$_2$), 161.0 (s, C-(CH$_2$CMe)=CH$_2$), 112.05 (s, C(*C*H$_2$CMe)=CH$_2$), 63.23 (d, $^2J_{PC}$ = 13.5 Hz, C=*C*H$_2$), 28.14 (s, C(CH$_2$*C*H$_3$)=CH$_2$).

$Fe_2(CO)_6(\mu\text{-}PPh_2)(\mu_2\text{-}\eta^1{:}\eta^2\text{-}C(C{\equiv}CPh){=}CHPh)$ (***11***). Obtained as orange red crystals in 84% yield from *n*-hexane at −10 °C. Anal. Calcd for $C_{28}H_{18}Fe_2O_6P$: C, 61.12; H, 3.17; P, 4.63. Found: C, 60.97; H, 3.44; P, 4.43. IR (ν(CO), cm^{-1}, C_6H_{12}): 2061 m, 2031 vs, 1998 s, 1984 s, 1951 vw, 1945 vw. ^1H NMR (200 MHz, $CDCl_3$, δ): 6.9–7.7 (m, C_6H_5, 20 H), 3.59 (d, $^3J_{PH}$ = 7.5 Hz, C=C*H*, 1 H), $^{31}P\{^1H\}$ NMR (81.02 MHz, $CDCl_3$, δ): 165.94 (s). $^{13}C\{^1H\}$ NMR (50.32 MHz, $CDCl_3$, δ): 210.4 (m, br, CO), 144.57 (d, $^2J_{PC}$ = 23.4

Hz, $C{=}CHC_6H_5$), 105.0 (s, $C{\equiv}CC_6H_5$), 101.63 (s, $C{\equiv}CC_6H_5$), 89.99 (d, $^3J_{PC}$ = 17.0 Hz, $C{=}CHC_6H_5$).

X-ray Structure Analyses of 5 and 10. Red crystals of **5** were grown from dichloromethane/hexane at −10 °C. Orange crystals of **10** were grown from a concentrated hexane solution at −10 °C. Suitable single crystals were chosen and mounted on glass fibers with epoxy resin. Unit-cell parameters were obtained for both crystals from least-squares refinements of the setting angles for 25 reflections well dispersed in reciprocal space.

Collection and Reduction of X-ray Data. Details of the intensity data collection are given in Table I. Data for **5** were collected at 295 K and for **10** at 180 K using graphite monochromated MoKα (λ = 0.71073 Å) radiation. Data for **5** and **10** were collected using the ω and θ–2θ scan methods, respectively, with a variable scan rate set to optimize measurements of weak reflections. Background measurements using the stationary crystal, stationary counter method were made at the beginning and end of each scan. Two standard reflections monitored every 100 reflections showed no significant changes (<2%) during the data collection. Measured reflections were flagged as unobserved when ($I \leq 6\sigma(F)$) where σ was derived from counting statistics.

Solution and Refinement of the Intensity Data. Patterson syntheses readily yielded positions for the two metal atoms in both cases and standard Fourier methods were used to locate the remaining atoms in the molecules. Full-matrix least-squares refinement of positional and isotropic thermal parameters and subsequent conversion to anisotropic coefficients for all non-hydrogen atoms and several further cycles of refinement gave R = 0.036 and 0.036 for **5** and **10**, respectively. At this stage a difference Fourier map revealed the positions of all the hydrogen atoms. In subsequent refinements to convergence, hydrogen atom positions and isotropic temperature coefficients were included. The function minimised in the least-squares calculations was $\sum w(|F_o| - |F_c|)^2$. The weighted R value is defined as $R_w = [\sum w(|F_o| - |F_c|)^2 / \sum w|F_o|^2]^{1/2}$, where the weights w, optimize on moderate intensities. Absorption corrections for **5** were applied by the face-indexed numerical procedure and an empirical absorption correction was applied for **10** based on a series of ψ scans. The atomic scattering factors used including anomalous dispersion corrections for iron were taken from the International Tables;[32] for hydrogen, those of Stewart et al. were used.[33] All calculations were performed on a Microvax II using SHELXTL PLUS software. The final R and R_w values together with the residual electron density levels are given in Table III.

Atomic positional parameters for **5** and **10** are listed in Tables IV and V respectively. Tables VI and VII contain appropriate selections of bond lengths and angles.

Acknowledgment. We thank Miss Janice Cramer (Department of Chemistry, McMaster University) for discussions regarding the spectroscopic observations. In addition we acknowledge the Natural Sciences and Engineering Research Council of Canada for financial support of this work (AJC).

Supplementary Material Available: For the structural analyses of both **5** and **10**, anisotropic thermal coefficients (Tables S1 and S5), remaining bond distances and angles (Tables S2 and S6), and hydrogen atom coordinates (Tables S3 and S7) (6 pages). Ordering information is given on any current masthead page. Structure factors (Tables S4 and S8, 33 pages) are available upon request from the authors.

OM9203136

(31) (a) Orpen, A. G.; Pippard, D.; Sheldrick, G. M.; Rouse, K. D. *Acta. Crystallogr., Sect. B* **1978**, *34*, 2466. (b) Iggo, J. A.; Mays, M. J.; Raithby, P. R.; Hendrick, K. *J. Chem. Soc., Dalton Trans.* **1983**, 205.

(32) *International Tables for X-ray Crystallography*; Kynoch Press: Birmingham, England, 1974; Vol. 4.

(33) Stewart, R. F.; Davidson, E. R.; Simpson, W. T. *J. Chem. Phys.* **1965**, *42*, 3175.